Commun Nonlinear Sci Numer Simulat 67 (2019) 203–222

Contents lists available at ScienceDirect

Commun Nonlinear Sci Numer Simulat

journal homepage: www.elsevier.com/locate/cnsns

Research paper

Mathematical assessment of the role of environmental factors on the dynamical transmission of cholera

G.G. Kolaye [a,b], S. Bowong [c,d,*], R. Houe [a,e], M.A. Aziz-Alaoui [f], M. Cadivel [f]

[a] Saint Jerome Polytechnic, Saint Jerome Catholic University Institute of Douala, Cameroon
[b] Department of Computer Sciences, Faculty of Science, University of Ngaoundere, PO Box 454, Ngaoundere, Cameroon
[c] Department of Computer Sciences, Faculty of Science, University of Douala, PO Box 24157, Douala, Cameroun
[d] UMI 209 IRD/UPMC UMMISCO, Bondy-France and Project GRIMCAPE, The African Center of Excellence in Information and Communication, Technologies (CETIC), University of Yaounde 1, Cameroon
[e] University of Toulouse, INPT, LGP-ENIT 47, avenue d'Azereix, BP 1629 F-65016, Tarbes Cedex, France
[f] Normandie Univ, UNIHAVRE, LMAH, FR-CNRS-3335, ISCN, Le Havre, 76600, France

ARTICLE INFO

Article history:
Received 3 August 2016
Revised 12 May 2018
Accepted 18 June 2018
Available online 20 August 2018

Keywords:
Cholera
Environmental reservoirs
Mathematical models
Stability
Sensitivity analysis

ABSTRACT

In this paper, we investigate the impact of environmental factors on the dynamical transmission of cholera within a human community. We propose a mathematical model for the dynamical transmission of cholera that incorporates the virulence of bacteria and the commensalism relationship between bacteria and the aquatic reservoirs on the persistence of the disease. We provide a theoretical study of the model. We derive the basic reproduction number $\mathcal{R}_0$ which determines the extinction and the persistence of the infection. We show that the disease-free equilibrium is globally asymptotically stable whenever $\mathcal{R}_0 \leq 1$, while when $\mathcal{R}_0 > 1$, the disease-free equilibrium is unstable and there exists a unique endemic equilibrium point which is locally asymptotically stable on a positively invariant region of the positive orthant. The sensitivity analysis of the model has been performed in order to determine the impact of related parameters on outbreak severity. Theoretical results are supported by numerical simulations, which further suggest the necessity to implement sanitation campaigns of aquatic environments by using suitable products against the bacteria during the periods of growth of aquatic reservoirs.

1. Introduction

Cholera was largely eliminated from industrialized countries by water and sewage treatment over a century ago. Today, it remains a significant cause of morbidity and mortality in developing countries, where it is a marker for inadequate drinking water and sanitation infrastructure. After several years of steady increase from 2007, the number of cholera cases reported by the World Health Organization (WHO), as well as the number of countries which reported cholera cases, showed a considerable decrease [1]. Yet, the disease is still a threat to many countries. For instance in 2012 alone, a cumulative total of 245,393 cases, including 3034 deaths with a case-fatality rate of 1.2%, were reported by WHO from all continents. This involves 48 countries among which, 27 from Africa, 12 from Asia, 6 from Americas and 3 from Europe and Oceania. Furthermore, the recent cholera outbreaks in the following countries led to a large number of infectious and deaths [1]:

* Corresponding author.
E-mail address: sbowong@gmail.com (S. Bowong).

https://doi.org/10.1016/j.cnsns.2018.06.023
1007-5704/

Angola (2012), Cameroon (2010–2012), Congo (2008, 2012), Haiti (2010–2011), India (2007), Iraq (2008, 2012), Kenya (2010), Nigeria (2010), Philippines (2012), UK (2012), Vietnam (2009) and Zimbabwe (2008–2009).

Vibrio cholerae (*V. cholerae*) is a Gram-negative, comma-shaped bacterium that causes cholera in humans. Cholera is an acute intestinal infection caused by the ingestion of contaminated foods and water with *V. cholerae* bacterium. Among the 200 serogroups of *V. cholerae*, only *V. cholerae* O1 and O139 are responsible of cholera disease [2]. The etiological agent passes through and survives the gastric acid barrier of the stomach and then penetrates the mucus lining that coats the epithelium [3]. Once they colonise the intestinal gut, they produce enterotoxin (which stimulates water and electrolyte secretion by the endothelial cells of the small intestine) that leads to watery diarrhea. If left untreated, it leads to death within hours. In human volunteer studies, the infection dose was determined to be $10^8 - 10^{11}$ cells [4]. Cholera is characterized, in its most severe form, by the sudden onset of acute watery diarrhea that can lead to death by severe dehydration. *V. cholerae* can stay in faeces without losing its infectious ability for 7–14 days and shed back to the environment. The main reservoirs of *V. cholerae* are people and aquatic sources.

It has been discovered that environmental aquatic bacteria such as *V. Cholerae* O1 and *V. cholerae* non-O1 have ability to survive to the stress caused by the variation of some environmental factors, such as temperature, pH or the lack of nutritional resources [5,6]. The adaptation of these bacteria to their environment will lead to metabolic and phenotypic changes that will condition their survival; what can be compared to a phenomenon of dormancy. Cells are considered “viable but non-culturable ” (VNC) because the main effect of this change is the loss of the ability to be cultivated on a bacteriological culture medium [7]. This dormancy state has been considered for many species of bacteria as a survival strategy in the natural environment [5,6,8–10]. The state change to the cultivable state is possible particularly if the factors causing stress become favorable to the development and growth of the bacterial population. This phenomenon implies to reconsider the thinking concerning the survival of pathogenic bacteria scattered into the environment and its dynamics in the aquatic ecosystem. This cell viability (VNC) is considered as a possible hypothesis at the origin of “disappearance” of the bacteria of the aquatic ecosystem during the colder months. Also, in the aquatic environment, *V. cholerae* has been reported to be associated with a variety of living organisms, including animals with an exoskeleton of chitin, aquatic plants, protozoa, bivalves, waterbirds, as well as abiotic substrates (e.g. sediments). Most of these are well-known or putative environmental reservoirs for the bacterium, defined as places where the pathogen lives over time, with the potential to be released and to cause human infection. Thus, the bacteria are strongly associated with the population of phytoplankton and zooplankton organisms forming commensal, antagonism, parasitism, competition, or symbiotic relationships. In this work, we will focus on the commensalism relationship between phytoplankton and *V. cholerae*. This commensalism relationship greatly enhances the bacterium’s ability to survive in an aquatic environment, as the exoskeleton provides the bacterium with an abundant source of carbon and nitrogen.

The dynamics of cholera are complex due to the multiple interactions between the human host and the pathogen in the water environment [8–19], which contributes to both direct and indirect transmission pathways. Many studies supported that V. cholerae O1 and O139 are commensal to crustacean zooplankton, notably copepods, which are present both in their gut and in biofilms on their chitinous surfaces [10–17]. Furthermore, V. cholerae is present throughout the year in and on its zooplankton host, and V. cholerae serogroup O1 has been shown to attach preferentially to zooplankton, but also to some species of phytoplankton in waters [16]. Its commensal existence provides protection from grazing by heterotrophic nanoflagellates and also from toxic chemicals, including those used to disinfect drinking water, such as alum and chlorine [17]. V. cholerae, like all Vibrio species, produces chitinase(s), with chitin serving as a nutrient source [18]. Also, Kirschner et al. demonstrated that association with zooplankton is important for V. cholerae non-O1/non-O139 serogroup isolates endemic in Neusiedler See, a large, shallow, moderately saline-alkaline lake in Central Europe [14]. A significant correlation was observed between the seasonal pattern in frequency of occurrence of V. cholerae and increased zooplankton biomass [14]. A deep understanding of the disease dynamics would have a significant impact on the effective prevention and control strategies [18,19]. Mathematical modeling and numerical simulations have the potential, and offer a promising way, to achieve this. Many efforts have been and are still being devoted to the modeling of this disease. For a chronological history of the modeling of cholera, we refer the reader to the work [21] which mentions the first mathematical model developed in [20–25]. Some theoretical studies have been carried out on the mathematical modeling of cholera transmission dynamics [26–29]. To our best knowledge, none of these mentioned works on cholera models have considered the change of metabolism of bacteria and the commensal relationships between bacteria and the population of phytoplankton and zooplankton.

In this paper, we explore the impact of environmental factors on the dynamical transmission of cholera within a human community. We formulate a mathematical model for cholera disease, which incorporates some key epidemiological and biological features of the disease such as the waning of recovery-induced immunity of recovered individuals, the virulence of bacteria and the commensal relationships between bacteria and the population of phytoplankton and zooplankton. We present the theoretical analysis of the model. We compute the disease-free equilibrium and derive the basic reproduction number $\mathcal{R}_0$ that depends on the rate of appearance and loss of virulence of bacteria and the carrying capacity of the population of phytoplankton and zooplankton. We do an in-depth analysis of the global asymptotic stability of the disease-free equilibrium and the local asymptotic asymptotical stability of the endemic equilibrium. The sensitivity analysis of the model is carried out to identify the most influential parameters on the model output variables, that is the most robust estimations that are required. Numerical simulations are presented to support the theory and to get insight on the role of the virulence of bacteria and the commensal relationship between bacteria and the population of phytoplankton and zooplankton on the

dynamics of the disease. Through numerical simulations, we found that the virulence of bacteria can increases the number of infected individuals and the mechanism of interaction between *V. cholerae* and environmental reservoirs would be the critical factor in the hatching of these bacteria in the environment.

The rest of the paper is organized as follows. After the formulation of the model in Section 2, we present its quantitative and qualitative analysis in Section 3. Numerical simulations are provided in Section 4. The last Section is devoted to concluding remarks on how our work fits in the literature.

2. Model formulation

We consider a heterogeneous population formed of humans, vibrio cholera and environmental reservoirs (i.e. the population of phytoplankton and zooplankton). The proposed model classifies the human population according to their disease status, namely: susceptible individuals S, symptomatic infected individuals with cholera I_1, asymptomatic infected individuals with cholera I_2 and recovered individuals R. Thus, the total human population at time t is given by

$$N(t) = S(t) + I_1(t) + I_2(t) + R(t). \tag{1}$$

The population of bacteria is divided into four subclasses with different properties: free virulent bacteria F_V (i.e. free in the environment and can infect susceptible individuals), free benign bacteria F_B (i.e. free in the water but cannot infect susceptible individuals), environmental virulent bacteria E_V (i.e. fixed in aquatic resources and can infect susceptible individuals) and environmental benign bacteria E_B (i.e. fixed in aquatic resources and cannot infect susceptible individuals). Thus, the total population of bacteria at time t is

$$B(t) = F_V(t) + F_B(t) + E_V(t) + E_B(t). \tag{2}$$

The populations of phytoplankton and zooplankton at time t is denoted by $P(t)$.

Susceptible individuals are recruited through birth and immigration at constant rate Λ. The source of infection is through oral ingestion of faecal contaminated water or food. Susceptible individuals may become infected either by contact with infected individuals or by ingestion of *V. Cholerae* content in the surrounding waters, infected fruits, vegetables and crustacean. Thus, the infection is regulated by the exposure with free pathogenic vibrios and infected water food at rates β_F and β_E per unit of time through the logistic dose-response $F_V/(F_V + K_F)$ and $E_V/(E_V + K_E)$ where K_F and K_E are respectively, the concentrations of free virulent and environmental virulent bacteria that yield 50% of chance for a susceptible individual to catch the infection [22]. Also, infected individual generates secondary infections through direct contact with susceptible individuals at rate $\beta_I(I_1 + I_2)/N$, where β_I is the human-to-human per capita contact rate per unit time. Thus, the force of infection is

$$\lambda = \beta_F \frac{F_V}{F_V + K_F} + \beta_E \frac{E_V}{E_V + K_E} + \beta_I \frac{I_1 + I_2}{N}. \tag{3}$$

We assume that a proportion p of newly infected individuals becomes symptomatic infected individuals and the complementary part $(1 - p)$ becomes asymptomatic infected individuals and enters the I_2 class. Once infected, asymptomatic and symptomatic individuals I_1 and I_2 can recover from the disease at constant rates r_1 and r_2, respectively. As suggested by many studies in the literature, recovered individuals may only have partial immunity [2,25,30,31]. Since the recover from the disease does not confer a total immunity to recovered individuals, recovered individuals loss their protection and return to the susceptible class S at rate δ. However, it is important to point out that there is no yet a vaccine inducing a long-term protection against cholera [31]. Infected individuals I_1 and I_2 contribute to the concentration of vibrios at constant rates α_1 and α_2, respectively. Susceptible, infected and recovered individuals have the same natural death rate μ_h. Symptomatic infected individuals die because of disease at constant rate d.

For the population of bacteria, when living conditions are unfavorable, pathogenic vibrios, i.e. those in the classes F_V and E_V become benign and enter the F_B and E_B classes at constant rates φ_b and θ_b, respectively. Also, when living conditions become favorable, benign bacteria, i.e. those in the F_B and E_B classes become pathogenic and move to the F_V and E_V classes at constant rates φ_v and θ_v, respectively. Pathogens are assumed to grow and decay at the same rates g and μ_b, respectively. Experimentally, it has been prove that $\mu_b > g$ [12]. We assume that free virulent and benign bacteria, i.e. those in the F_V and F_B classes become environmental virulent and benign bacteria (i.e. those in the E_V and E_B classes) by clinging on the population of phytoplankton and zooplankton at rate $\eta P/(Q_f + P)$ where η is the force of commensalism of environmental virulent and benign bacteria with respect to the population of phytoplankton and zooplankton per unit of time and Q_f a positive constant. Without loss of generality, we assume that a proportion ε of environmental bacteria (i.e. those in the E_V and E_B classes) takes advantage of their association with the populations of phytoplankton and zooplankton to face stress caused by climatic conditions. Thus, the environmental virulent and benign bacteria survive at rate $\varepsilon(\mu_b - g)$ du to their commensal relationship with the populations of phytoplankton and zooplankton. We assume that the population of phytoplankton and zooplankton experiences a logistic growth with a carrying capacity M_p and maximum growth rate r.

The structure of the model is shown in Fig. 1. The dashed arrow indicates contamination of the environment by infected humans.

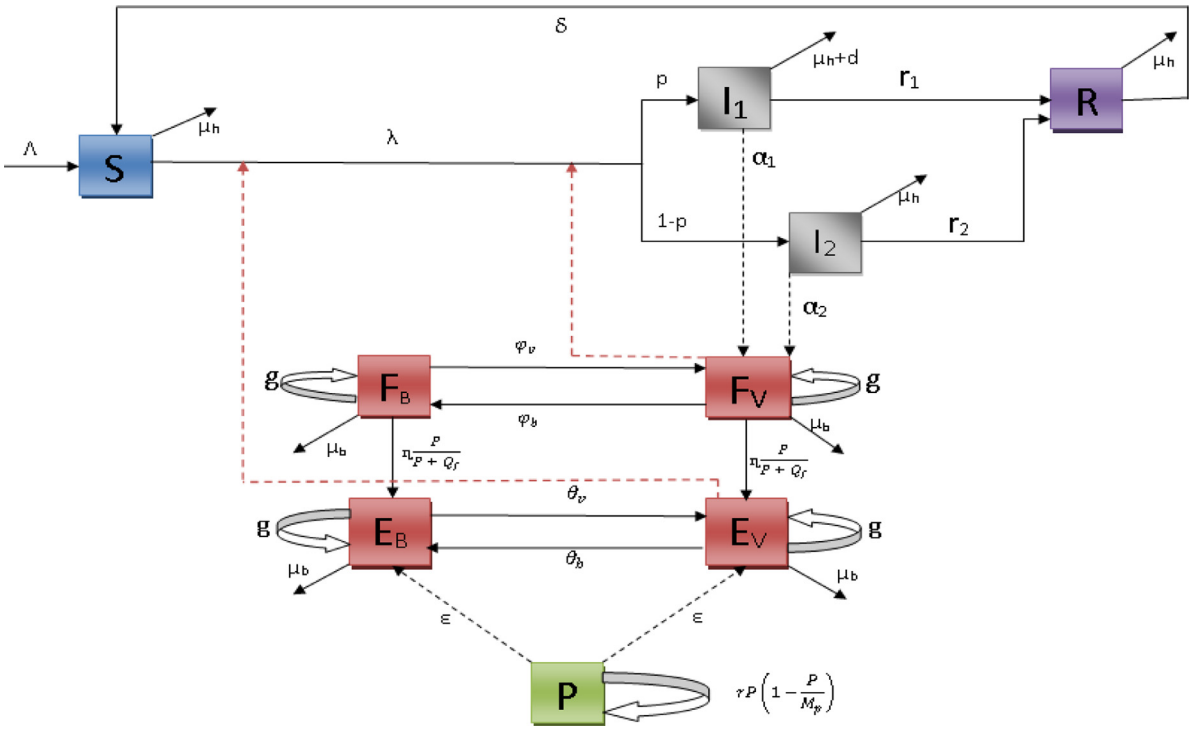

Fig. 1. Flow chart of the transmission dynamics of the cholera model.

The dynamics of the disease can be described by the following system of non linear differential equations:

$$\begin{cases} \dot{S} &= \Lambda + \delta R - (\lambda + \mu_h)S, \\ \dot{I}_1 &= p\lambda S - (\mu_h + r_1 + d)I_1, \\ \dot{I}_2 &= (1-p)\lambda S - (\mu_h + r_2)I_2, \\ \dot{R} &= r_1 I_1 + r_2 I_2 - (\delta + \mu_h)R, \\ \dot{F}_V &= \alpha_1 I_1 + \alpha_2 I_2 + \varphi_v F_B - \left(D_1 + \varphi_b + \eta \frac{P}{Q_f+P}\right)F_V, \\ \dot{F}_B &= \varphi_b F_V - \left(D_1 + \varphi_v + \eta \frac{P}{Q_f+P}\right)F_B, \\ \dot{E}_V &= \eta \frac{P}{Q_f+P} F_V + \theta_v E_B - (D_2 + \theta_b)E_V, \\ \dot{E}_B &= \eta \frac{P}{Q_f+P} F_B + \theta_b E_V - (D_2 + \theta_v)E_B, \\ \dot{P} &= rP(1 - \frac{P}{M_p}), \end{cases} \tag{4}$$

where λ is defined as in Eq. (3), $D_1 = \mu_b - g$ and $D_2 = D_1\epsilon$.

First of all, let us recall some useful results that we will use in the sequel.

Definition 1. Consider the following systems in $x \in \mathbb{R}^n$:

$$\dot{x} = f(t, x), \tag{5}$$

$$\dot{y} = g(y), \tag{6}$$

where f and g are continuous and locally Lipschitz functions in x so that the solutions exist for all $t \geq 0$. System (5) is called asymptotically autonomous with limit system (6) if $f(t, x) \to g(y)$ as $t \to \infty$ uniformly in $x \in \mathbb{R}^n$.

Lemma 1 [32]. *Let x_e be a locally asymptotically stable equilibrium of (6) and ω the ω-limit set of a forward bounded solution $x(t)$ of (5). If ω contains a point y_0 such that the solution y of (6), with $y(0) = y_0$ converges to x_e as $t \to \infty$, then $\omega = \{x_e\}$, i.e. $x(t) \to x_e$ as $t \to \infty$.*

Corollary 1 [32]. *If the solutions of system (5) are bounded and the equilibrium x_e of the limit system (6) is globally asymptotically stable, then every solution $x(t)$ of the system (5) satisfies $x(t) \to x_e$ as $t \to \infty$.*

Table 1
Numerical values for the parameters of model system (4).

Definition	Symbols	Estimated	Source
Recruitment rate	Λ	28 day^{-1}	Assumed
Exposure rate to infected people	β_I	0.005 person^{-1}day^{-1}	Assumed
Exposure rate to infected waters	β_F	0.002 person $^{-1}$day^{-1}	Assumed
Exposure rate to infected water's foods infected	β_E	0.001 person^{-1}day^{-1}	Assumed
Proportion of symptomatic infected human	p	0.2	[25]
Waning rate of treatment induced-immunity	δ	0.00092 day^{-1}	[30]
Natural mortality rate of humans	μ_h	0.0104 day^{-1}	[33]
Cholera induced mortality	d	0.046 day^{-1}	[34]
Recovery rate of symptomatic infected individuals	r_1	0.045 day^{-1}	[35]
Recovery rate of asymptomatic infected individuals	r_2	0.0045 day^{-1}	Assumed
Pathogen shed rate of symptomatic infected individuals	α_1	70 Cells day^{-1} person^{-1}	[25]
Pathogen shed rate of asymptomatic infected individuals	α_2	10 Cells day^{-1} person^{-1}	[25]
Decay rate of pathogens	μ_b	1.06 day^{-1}	[22]
Growth rate of pathogens	g	0.73 day^{-1}	[22]
Proportion of environmental bacteria that survives	ε	0.7	Assumed
Commensalism force of environmental bacteria	η	0.05 day^{-1} reservoir^{-1}	Assumed
Carrying capacity of the aquatic environment	M_p	10^{10}	Assumed
Concentration of free *V. Cholerae* in water	K_F	10^4	Assumed
Concentration of environmental *V. Cholerae* in water	K_E	10^6	[22]
Half of number of infected reservoirs	Q_f	10^5	Assumed
Growth rate of reservoirs	r	0.01 day^{-1}	Assumed
Rate at which benign bacteria becomes virulent bacteria	φ_v	0.05 day^{-1}	Assumed
Rate at which virulent bacteria becomes benign bacteria	φ_b	0.008 day^{-1}	Assumed
Rate at which environmental benign bacteria become environmental virulent bacteria	θ_v	0.08 day^{-1}	Assumed
Rate at which environmental virulent bacteria become environmental benign bacteria	θ_b	0.005 day^{-1}	Assumed

Since $P^* = M_p$ is a globally asymptotically stable equlibrium of the population dynamics of phytoplankton and zooplankton $\dot{P} = rP(1 - \frac{P}{M_p})$ then $P(t) \to M_p$ as $t \to +\infty$ uniformly. Therefore, from Lemma 1 and Corollary 1, model system (4) is reduced to

$$\begin{cases} \dot{S} &= \Lambda + \delta R - (\lambda + \mu_h)S, \\ \dot{I}_1 &= p_1\lambda S - \omega_1 I_1, \\ \dot{I}_2 &= p_2\lambda S - \omega_2 I_2, \\ \dot{R} &= r_1 I_1 + r_2 I_2 - (\delta + \mu_h)R, \\ \dot{F}_V &= \alpha_1 I_1 + \alpha_2 I_2 + \varphi_v F_B - \left(\varphi_b + \Sigma_\eta + D_1\right)F_V, \\ \dot{F}_B &= \varphi_b F_V - \left(\varphi_v + \Sigma_\eta + D_1\right)F_B, \\ \dot{E}_V &= \Sigma_\eta F_V + \theta_v E_B - (\theta_b + D_2)E_V, \\ \dot{E}_B &= \Sigma_\eta F_B + \theta_b E_V - (\theta_v + D_2)E_B, \end{cases} \tag{7}$$

where $p_1 = p,\ p_2 = 1 - p,\ \omega_1 = \mu_h + r_1 + d\ ,\ \omega_2 = \mu_h + r_2$ and $\Sigma_\eta = \eta\frac{M_p}{Q_f + M_p}$.

The parameter values used for numerical simulations are given in Table 1.

3. Mathematical analysis

3.1. Basic properties

3.1.1. Positivity of solutions

We investigate the asymptotic behavior of orbits starting in the nonnegative cone $\mathbb{R}^8_+$. Obviously, model system (7) which is a C^∞ differential system, admits a unique maximal solution for any associated Cauchy problem.

Theorem 1. *Let* $(t_0 = 0,\ X_0 = (S(0), I_1(0), I_2(0), R(0), F_V(0), F_B(0), E_V(0))) \in \mathbb{R} \times \mathbb{R}^8_+$ *and for* $T \in]0, +\infty]$, $([0, T[,\ X = (S(t), I_1(t), I_2(t), R(t), F_V(t), F_B(t), E_V(t), E_B(t)))$ *the maximal solution of the Cauchy problem associated to model system* (7). *Then,* $\forall t \in [0;\ T[,\ X(t) \in \mathbb{R}^8_+$

Proof. Let

$$\Delta = \Big\{\tilde{t} \in [0; T[\ \mid S(t) > 0,\ I_1(t) > 0,\ I_2(t) > 0,\ R(t) > 0,\ F_V(t) > 0,$$

$$F_B(t) > 0,\ E_V(t) > 0 \text{ and } E_B(t) > 0\ \ \forall t \in]0,\ \tilde{t}[\Big\}.$$

By continuity of function S, I_1, I_2, R, F_V, F_B, E_V and E_B, one can see that $\Delta \neq \emptyset$. Let $\tilde{T} = \sup\Delta$. Now, we are going to show that $\tilde{T} = T$. Suppose $\tilde{T} < T$, then one has that S, I_1, I_2, R, F_V, F_B, E_V and E_B are non negative on $[0; \tilde{T}[$. At $\tilde{T}$, at least one of

the following conditions is satisfied $S(\tilde{T}) = 0$, $I_1(\tilde{T}) = 0$, $I_2(\tilde{T}) = 0$, $R(\tilde{T}) = 0$, $F_V(\tilde{T}) = 0$, $F_B(\tilde{T}) = 0$, $E_V(\tilde{T}) = 0$ and $E_B(\tilde{T}) = 0$. Suppose $S(\tilde{T}) = 0$, then from the first equation of model system (7), one has

$$\frac{d}{dt}\left(Se^{\int_0^t(\lambda(r)+\mu_h)dr}\right) = (\Lambda + \delta R)e^{\int_0^t(\lambda(r)+\mu_h)dr}. \tag{8}$$

Integrating Eq. (8) from 0 to $\tilde{T}$ yields

$$S(\tilde{T}) = e^{-\int_0^{\tilde{T}}(\lambda(r)+\mu_h)dr}\left(S(0) + \int_0^{\tilde{T}}\left(e^{\int_0^t(\lambda(r)+\mu_h)dr}\right).(\Lambda + \delta R(t))dt\right) > 0.$$

Similarly, one can show that $I_1(\tilde{T}) > 0$, $I_2(\tilde{T}) > 0$, $R(\tilde{T}) > 0$, $F_V(\tilde{T}) > 0$, $F_B(\tilde{T}) > 0$, $E_V(\tilde{T}) > 0$ and $E_B(\tilde{T}) > 0$. This is a contradiction. Then, $\tilde{T} = T$ and consequently the maximal solution $(S(t), I_1(t), I_2(t), R(t), F_V(t), F_B(t), E_V(t), E_B(t))^T$ of the Cauchy problem associated to model system (7) is positive. This achieves the proof. □

3.1.2. Invariant region

We first split model system (7) into two parts, the human population (i.e. $S(t)$, $I_1(t)$, $I_2(t)$ and $R(t)$) and the pathogen population (i.e. $F_V(t)$, $F_B(t)$, $E_V(t)$ and $E_B(t)$). Then, using model system (7), the dynamics of the total human population satisfy

$$\dot{N} = \Lambda - \mu_h N - dI_1 \leq \Lambda - \mu_h N. \tag{9}$$

Integrating the above differential inequality yields

$$0 \leq N(t) \leq \frac{\Lambda}{\mu_h} + \left(N(0) - \frac{\Lambda}{\mu_h}\right)e^{-\mu_h t}, \qquad \forall t \geq 0,$$

where $N(0)$ is the initial value of $N(t)$. It implies that $0 \leq N(t) \leq \frac{\Lambda}{\mu}$ for all $t \geq 0$ if $N(0) \leq \frac{\Lambda}{\mu}$. Now, using the fact that $I_1(t) \leq \Lambda/\mu_h$ and $I_2(t) \leq \Lambda/\mu_h$, the dynamics of bacteria satisfies

$$\dot{B} \leq \alpha\frac{\Lambda}{\mu_h} - \xi B, \tag{10}$$

where $\alpha = \max\{\alpha_1, \alpha_2\}$ and $\xi = \min\{D_1, D_2\}$. Integrating Eq. (10) gives

$$0 \leq B(t) \leq \frac{\alpha\Lambda}{\xi\mu_h} + \left(B(0) - \frac{\alpha\Lambda}{\xi\mu_h}\right)e^{-\xi t}, \qquad \forall t \geq 0,$$

where $B(0)$ represents the initial value of $B(t)$. It then follows that $B(t) \leq \frac{\alpha\Lambda}{\xi\mu_h}$ for all $t \geq 0$ if $B(0) \leq \frac{\alpha\Lambda}{\xi\mu_h}$. Thus, the region:

$$\Omega = \left\{(S, I_1, I_2, R, F_V, F_B, E_V, E_B) \in \mathbb{R}^8_+, \quad N \leq \frac{\Lambda}{\mu_h} \quad \text{and} \quad B \leq \frac{\alpha\Lambda}{\xi\mu_h}\right\}, \tag{11}$$

is positively invariant and attracting for model system (7). Then, it is sufficient to consider the dynamics of the flow generated by model system (7) in Ω.

Remark 1. Every maximal solution of model system (7) are global.

3.2. Disease-free equilibrium and its stability

Model system (7) has a disease-free equilibrium obtained by setting the right-hand side of equations in model system (7) to zero with $I_1 = I_2 = 0$. The disease-free equilibrium is

$$Q_0 = (S_0, 0, 0, 0, 0, 0, 0, 0), \tag{12}$$

where $S_0 = \frac{\Lambda}{\mu_h}$.

The linear stability of Q_0 is governed by the basic reproductive number [36,37]. The stability of this equilibrium will be investigated using the next generation operator [38,39]. Using the notations in van den Driessche and Watmough [39,40] for model system (7), the Jacobian matrices F and V at the DFE for the new infection and remaining transfer terms are, respectively given by

$$F = \begin{bmatrix} p_1\beta_I & p_1\beta_I & p_1S_0\frac{\beta_F}{K_F} & 0 & p_1S_0\frac{\beta_E}{K_E} & 0 \\ p_2\beta_I & p_2\beta_I & p_2S_0\frac{\beta_F}{K_F} & 0 & p_2S_0\frac{\beta_E}{K_E} & 0 \\ 0 & 0 & 0 & 0 & 0 & 0 \\ 0 & 0 & 0 & 0 & 0 & 0 \\ 0 & 0 & 0 & 0 & 0 & 0 \\ 0 & 0 & 0 & 0 & 0 & 0 \end{bmatrix} V = \begin{bmatrix} \omega_1 & 0 & 0 & 0 & 0 & 0 \\ 0 & \omega_2 & 0 & 0 & 0 & 0 \\ -\alpha_1 & -\alpha_2 & M_b & -\varphi_v & 0 & 0 \\ 0 & 0 & -\varphi_b & M_v & 0 & 0 \\ 0 & 0 & -\Sigma_\eta & 0 & N_b & -\theta_v \\ 0 & 0 & 0 & -\Sigma_\eta & -\theta_b & N_v \end{bmatrix},$$

where $M_b = \varphi_b + \Sigma_\eta + D_1$, $M_v = \varphi_v + \Sigma_\eta + D_1$, $N_v = \theta_v + D_2$ and $N_b = \theta_b + D_2$.

Following Van den Driessche and Watmough [39], the basic reproduction number of model system (7) is

$$\mathcal{R}_0 = \rho(FV^{-1}) = \mathcal{R}_{01} + \mathcal{R}_{02}, \tag{13}$$

where $\rho(FV^{-1})$ is the spectral radius of the next generation matrix FV^{-1}, $\mathcal{R}_{01}$ and $\mathcal{R}_{02}$ are respectively, the symptomatic infection and asymptomatic infection induced basic reproduction numbers given by

$$\mathcal{R}_{0i} = \beta_I \frac{p_i}{\omega_i} + \beta_F \frac{p_i \alpha_i S_0 \left(\varphi_v + \Sigma_\eta + D_1\right)}{\omega_i K_F \left(\Sigma_\eta + D_1\right)\left(\Sigma_\eta + D_1 + \varphi_b + \varphi_v\right)} \tag{14}$$

$$+\beta_E \frac{p_i \alpha_i S_0 \Sigma_\eta \left[\left(\varphi_v + \Sigma_\eta + D_1\right)(\theta_v + D_2) + \varphi_b \theta_v\right]}{\omega_i K_E D_2 (D_2 + \theta_b + \theta_v)\left(\Sigma_\eta + D_1\right)\left(\Sigma_\eta + D_1 + \varphi_b + \varphi_v\right)}, \qquad i \in \{1, 2\}. \tag{14}$$

The threshold quantity $\mathcal{R}_0$ measures the average number of new cholera infections generated by a single infective in a completely susceptible population without any intervention.

The relevance of the reproduction number is due to the following result established from Theorem 2 in [39].

Lemma 2. *The disease-free equilibrium* Q_0 *of model system (7) is locally asymptotically stable in* Ω *whenever* $\mathcal{R}_0 \leq 1$ *and unstable whenever* $\mathcal{R}_0 > 1$.

The biological implication of Lemma 2 is that a sufficiently small flow of infectious individuals will not generate outbreak of the disease unless $\mathcal{R}_0 > 1$. For a better control on the disease, the global asymptotic stability (GAS) of the DFE is needed. Actually, enlarging the basin of attraction of Q_0 to be the entire Ω is, for the model under consideration a more challenging task involving relatively new result. We use the result of Kamgang and Sallet [41,50] for the global stability of the disease-free equilibrium for a class of epidemiological models.

Using the result of Kamgang and Sallet [50], model system (7) can be written in the following form:

$$\begin{cases} \dot{x}_s = A_1(x)(x_s - x_s^0) + A_{12}(x)x_i, \\ \dot{x}_i = A_2(x)x_i, \end{cases} \tag{15}$$

where $x_s = (S, R)^T$ represents the class of non infected individuals (i.e. susceptible and recovered individuals), $x_i = (I_1, I_2, F_V, F_B, E_V, E_B)^T$ represents the class of infected individuals (i.e. symptomatic infected individuals, asymptomatic infected individuals, virulent-free bacteria, benign-free bacteria, virulent-environmental bacteria and benign-environmental bacteria), $x = (x_s, x_i)^T$ and $x_s^0 = (S_0, 0)$ with S_0 the non zero component of the disease-free equilibrium. Matrice $A_1(x)$, $A_{12}(x)$ and $A_2(x)$ in Eq. (15) are defined by

$$A_1(x) = \begin{bmatrix} -(\mu_h + \lambda) & \delta \\ 0 & -(\delta + \mu_h) \end{bmatrix}, \qquad A_{12}(x) = \begin{bmatrix} -\frac{\beta_I S_0}{N} & -\frac{\beta_I S_0}{N} & -\frac{\beta_F S_0}{F_V + K_F} & 0 & -\frac{\beta_F S_0}{E_V + K_E} & 0 \\ r_1 & r_1 & 0 & 0 & 0 & 0 \end{bmatrix}$$

and

$$A_2(x) = \begin{bmatrix} -\omega_1 + \frac{p_1 \beta_I S}{N} & \frac{p_1 \beta_I S}{N} & \frac{p_1 \beta_F S}{F_V + K_F} & 0 & \frac{p_1 \beta_E S}{E_V + K_E} & 0 \\ \frac{p_2 \beta_I S}{N} & -\omega_2 + \frac{p_2 \beta_I S}{N} & \frac{p_2 \beta_F S}{F_V + K_F} & 0 & \frac{p_2 \beta_E S}{E_V + K_E} & 0 \\ \alpha_1 & \alpha_2 & -\varphi_b - \Sigma_\eta - D_1 & \varphi_v & 0 & 0 \\ 0 & 0 & \varphi_b & -\varphi_v - \Sigma_\eta - D_1 & 0 & 0 \\ 0 & 0 & \Sigma_\eta & 0 & -\theta_b - D_2 & \theta_v \\ 0 & 0 & 0 & \Sigma_\eta & \theta_b & -\theta_v - D_2 \end{bmatrix}.$$

The conditions $H_1 - H_5$ below must be met to guarantee the global asymptotic stability (GAS) of Q_0.

- H_1: Model system (15) is defined on a positively invariant set $\mathcal{D}$ of the nonnegative orthant. Model system (15) is dissipative on $\mathcal{D}$.
- H_2: The sub-system $\dot{x}_s = A_1(x_s, 0)(x_s - x_s^0)$ is globally asymptotically stable at the equilibrium x_s^0 on the canonical projection of $\mathcal{D}$ on $\mathbb{R}^2_+$.
- H_3: The matrix $A_2(x)$ is Metzler (A Metzler matrix is a matrix with off-diagonal entries nonnegative [33,35]) and irreducible for any given $x \in \mathcal{D}$.
- H_4: There exists an upper-bound matrix $\overline{A_2}$ for $\mathcal{M} = \{A_2(x) \mid x \in \mathcal{D}\}$ with the property that either: $\overline{A_2} \notin \mathcal{M}$ or if $\overline{A_2} \in M$ then for any $x \in \mathcal{D}$ such that $\overline{A_2} = A_2(x)$, $x \in \mathbb{R}^2_+ \times \{0\}$ (i.e. the points where the maximum is realized are contained in the disease-free sub-manifold).
- H_5: $\rho(\overline{A_2}) \leq 0$ where $\rho(\overline{A_2})$ denotes the largest real part of the eigenvalues of $\overline{A_2}$.

The result of Kamgang–Sallet approach [50] uses the algebraic structure of model system (15), namely the fact that $A_1(x)$ and $A_2(x)$ are Metzler matrices. Since in the said approach the matrix $A_2(x)$ is required to be irreducible, we further restrict the domain of the system to:

$$\mathcal{D} = \{(x_s, x_i) \in \Omega, \quad x_s \neq 0\}. \tag{16}$$

The set $\mathcal{D}$ is positively invariant because only the initial point of any trajectory can have $x_s = 0$ (see Theorem 1). Indeed, from the first and fourth equations of model system (7), one has $S' > 0$ and $R' > 0$ whenever $S = 0$ and $R = 0$. Therefore, we restrict the domain of system (15) to $\mathcal{D}$ where $A_2(x)$ irreducible. Thus, one has that

$$A_2(x) \text{ is Metzler and irreducible for all } x \in \mathcal{D}. \tag{17}$$

The sub-system:

$$\dot{x}_s = A_1(x_s, 0)(x_s - x_s^0),$$

is equivalent to

$$\begin{cases} \dot{S} = \Lambda + \delta R - \mu_h S, \\ \dot{R} = -(\delta + \mu_h) R. \end{cases} \tag{18}$$

Resolving the above equations and taking the limit of solutions when t go to infinity yields

$$\lim_{t \to +\infty} S(t) = \frac{\Lambda}{\mu} \qquad \text{and} \qquad \lim_{t \to +\infty} R(t) = 0.$$

Therefore,

$$\begin{aligned} &x_s^0 = (S_0, 0) \text{ is a globally asymptotically stable equilibrium of the} \\ &\text{reduced system (18) on the sub-domain} \mathcal{D}. \end{aligned} \tag{19}$$

Then, the hypothesis $\boldsymbol{H_2}$ is satisfied.

The theorem of Kamgang and Sallet (see [50], Theorem 4.3) gives the GAS of the DFE of a dissipative system of the form (15) which satisfies (17) and (19) provided there exists a matrix $A_2(x)$ with the following additional properties:

$$\begin{cases} A_2(x) \leq \bar{A}_2, \quad x \in \mathcal{D}, \\ \text{if} \quad A_2(\bar{x}) = \bar{A}_2 \quad \text{for some} \quad \bar{x} = (\bar{x}_1, \bar{x}_2)^T \in \mathcal{D} \quad \text{then} \quad \bar{x}_2 = 0, \\ \alpha(\bar{A}_2) \leq 0. \end{cases} \tag{20}$$

The equality $A_2(x) = \bar{A}_2$ is possible only when $S = N = S_0$ and $F_v = E_v = 0$ which implies that $x_i = 0$. Therefore, the first and second conditions in (20) hold. Note that $\bar{A}_2$ is a Metzler matrix which satisfies the stability condition of Kamgang and Sallet [50].

Now, using the fact that $\frac{S}{N} \leq 1$, $\frac{S}{F_V + K_F} \leq \frac{S_0}{K_F}$ and $\frac{S}{E_V + K_E} \leq \frac{S_0}{K_E}$, one has

$$\overline{A_2} = \begin{bmatrix} -\omega_1 + p_1\beta_I & p_1\beta_I & \frac{p_1\beta_F S_0}{K_F} & 0 & \frac{p_1\beta_E S}{K_E} & 0 \\ p_2\beta_I & -\omega_2 + p_2\beta_I & \frac{p_2\beta_F S_0}{K_F} & 0 & \frac{p_2\beta_E S_0}{K_E} & 0 \\ \alpha_1 & \alpha_2 & -\varphi_b - \Sigma_\eta - D_1 & \varphi_v & 0 & 0 \\ 0 & 0 & \varphi_b & -\varphi_v - \Sigma_\eta - D_1 & 0 & 0 \\ 0 & 0 & \Sigma_\eta & 0 & -\theta_b - D_2 & \theta_v \\ 0 & 0 & 0 & \Sigma_\eta & \theta_b & -\theta_v - D_2 \end{bmatrix}.$$

From the above expression of $\bar{A}_2$, one can observe that there is a maximum which is uniquely realized in $\mathcal{D}$ at Q_0 and this maximum is then the block of the Jacobian of model system (15) at the disease-free equilibrium Q_0, corresponding to the matrix $A_2(x)$, and the condition $\boldsymbol{H_4}$ is satisfied.

Now, we check the condition H_5. Note that the condition $\rho(\overline{A_2}) \leq 0$ implies that $\overline{A_2}$ is a stable Metzler matrix. We show in Appendix A that the condition $\rho(\overline{A_2}) \leq 0$ is equivalent to $\mathcal{R}_0 \leq 1$.

We can now apply Theorem 4.3 in Kamgang and Sallet [50] and conclude that the disease-free equilibrium $(x_s^0, 0)$ is GAS in $\mathcal{D}$. From Eq. (16), for the points of $\mathcal{D}$ where $x_s = 0$, and the disease-free equilibrium is GAS on Ω.

We have established the following result about the global stability of the disease-free equilibrium Q_0.

Theorem 2. *The disease-free equilibrium point Q_0 of model system (7) is globally asymptotically stable in Ω if $\mathcal{R}_0 < 1$ and unstable if $\mathcal{R}_0 > 1$.*

3.3. Endemic equilibrium and its stability

Let $Q^* = \left(S^*, I_1^*, I_2^*, R^*, F_V^*, F_B^*, E_V^*, E_B^*\right)$ be any endemic equilibrium (EE) of model system (7) with $S^* \neq 0$, $I_1^* \neq 0$, $I_2^* \neq 0$, $R^* \neq 0$, $F_V^* \neq 0$, $F_B^* \neq 0$, $E_V^* \neq 0$ and $E_B^* \neq 0$ satisfying the following system of equations:

$$\begin{cases} \Lambda + \delta R^* - (\lambda^* + \mu_h)S^* = 0, \\ p_1\lambda^* S^* - \omega_1 {I^*}_1 = 0, \\ p_2\lambda^* S^* - \omega_2 {I^*}_2 = 0, \\ r_1 {I^*}_1 + r_2 {I^*}_2 - (\delta + \mu_h)R^* = 0, \\ \alpha_1 {I^*}_1 + \alpha_2 {I^*}_2 + \varphi_v {F^*}_B - \left(\varphi_b + \Sigma_\eta + D_1\right){F^*}_V = 0, \\ \varphi_b {F^*}_V - \left(\varphi_v + \Sigma_\eta + D_1\right){F^*}_B = 0, \\ \Sigma_\eta {F^*}_V + \theta_v {E^*}_B - (\theta_b + D_2){E^*}_V = 0, \\ \Sigma_\eta {F^*}_B + \theta_b {E^*}_V - (\theta_v + D_2){E^*}_B = 0, \end{cases} \tag{21}$$

where

$$\lambda^* = \beta_F \frac{F_V^*}{F_V^* + K_F} + \beta_E \frac{E_V^*}{E_V^* + K_E} + \beta_I \frac{I_1^* + I_2^*}{S^* + R^* + I_1^* + I_2^*}, \tag{22}$$

is the force of infection at the endemic steady state.

Expressing the endemic states $S^*, I_2^*, R^*, F_V^*, F_B^*, E_V^*$ and E_B^* as a function of I_1^* and λ^* gives

$$\begin{aligned} S^* &= \frac{\Lambda}{\lambda^* + \mu_h} + \delta \frac{r_1\omega_2 p_1 + r_2\omega_1 p_2}{(\lambda^* + \mu_h)(\delta + \mu_h)} I_1^*, \qquad I_2^* = \frac{\omega_1 p_2}{\omega_2 p_1} I_1^* \qquad R^* = \frac{r_1\omega_2 p_1 + r_2\omega_1 p_2}{(\lambda^* + \mu_h)(\delta + \mu_h)} I_1^*, \\ F_V^* &= \frac{\left(\varphi_v + \Sigma_\eta + D_1\right)(\alpha_1\omega_2 p_1 + \alpha_2\omega_1 p_2)}{\omega_2 p_1\left(\Sigma_\eta + D_1\right)\left(\Sigma_\eta + D_1 + \varphi_b + \varphi_v\right)} I_1^*, \qquad F_B^* = \frac{\varphi_b(\alpha_1\omega_2 p_1 + \alpha_2\omega_1 p_2)}{\omega_2 p_1\left(\Sigma_\eta + D_1\right)\left(\Sigma_\eta + D_1 + \varphi_b + \varphi_v\right)} I_1^*, \\ E_V^* &= \frac{\Sigma_\eta\left(\theta_v\varphi_b + (\theta_v + D_2)\left(\varphi_v + \Sigma_\eta + D_1\right)\right)(\alpha_1\omega_2 p_1 + \alpha_2\omega_1 p_2)}{D_2(D_2 + \theta_b + \theta_v)\left(\Sigma_\eta + D_1\right)\left(\Sigma_\eta + D_1 + \varphi_b + \varphi_v\right)\omega_2 p_1} I_1^* \qquad \text{and} \\ E_B^* &= \left(\varphi_b + \frac{\theta_b\left(\theta_v\varphi_b + (\theta_v + D_2)\left(\varphi_v + \Sigma_\eta + D_1\right)\right)}{D_2(D_2 + \theta_b + \theta_v)}\right) \frac{\Sigma_\eta(\alpha_1\omega_2 p_1 + \alpha_2\omega_1 p_2)}{(\theta_v + D_2)\omega_2 p_1\left(\Sigma_\eta + D_1\right)\left(\Sigma_\eta + D_1 + \varphi_b + \varphi_v\right)} I_1^*. \end{aligned} \tag{23}$$

From the second equation of (23), using the expression of S^* defined as in Eq. (23), one has

$$I_1^* = \frac{\lambda^* p_1 \Lambda(\delta + \mu_h)}{\lambda^*\left[w_1\left(\delta\left(1 - \frac{r_1 p_1}{\omega_1} - \frac{r_2 p_2}{\omega_2}\right) + \mu_h\right)\right] + \omega_1\mu_h(\mu_h + \delta)} > 0, \tag{24}$$

because $1 - \frac{r_1 p_1}{\omega_1} - \frac{r_2 p_2}{\omega_2} \geq 0$. Now, after plugging Eqs. (21) and (24) into Eq. (22), one obtains the following fourth order polynomial equation in λ^*:

$$c_4(\lambda^*)^4 + c_3(\lambda^*)^3 + c_2(\lambda^*)^2 + c_1(\lambda^*) + c_0 = 0, \tag{25}$$

where

$$\begin{cases} c_0 &= \Lambda c a_{10}(1 - \mathcal{R}_0), \\ c_1 &= a_{10}c\Lambda + a_4 a_{11} - \beta_I a a_1 a_{10} - \beta_I \mu_h a a_1 a_4, \\ c_2 &= c\Lambda a_5 a_6 + a_4 a_{10} + a a_1 a_{11} - \beta_I a a_1 a_9 - \beta_I \mu_h a a_1 a_5 a_6, \\ c_3 &= a_5 a_6 a_4 + a a_1 a_{10} - \beta_I a a_1 a_5 a_6, \\ c_4 &= a a_1 a_5 a_6, \end{cases}$$

with

$$\begin{aligned} &a = p_1\Lambda(\delta + \mu_h), \qquad b = \left[w_1\left(\delta\left(1 - \tfrac{r_1 p_1}{\omega_1} - \tfrac{r_2 p_2}{\omega_2}\right) + \mu_h\right)\right], \qquad c = \omega_1\mu_h(\mu_h + \delta), \\ &L_F = \frac{K_F\omega_2 p_1\left(\Sigma_\eta + D_1\right)\left(\Sigma_\eta + D_1 + \varphi_b + \varphi_v\right)}{\left(\varphi_v + \Sigma_\eta + D_1\right)(\alpha_1\omega_2 p_1 + \alpha_2\omega_1 p_2)}, \\ &L_E = \frac{K_E D_2(D_2 + \theta_b + \theta_v)\left(\Sigma_\eta + D_1\right)\left(\Sigma_\eta + D_1 + \varphi_b + \varphi_v\right)\omega_2 p_1}{\Sigma_\eta\left(\theta_v\varphi_b + (\theta_v + D_2)\left(\varphi_v + \Sigma_\eta + D_1\right)\right)(\alpha_1\omega_2 p_1 + \alpha_2\omega_1 p_2)}, \end{aligned}$$

$$\begin{aligned} &a_1 = \frac{\omega_1 p_2}{\omega_2 p_1} + 1, \qquad a_2 = \frac{r_1\omega_2 p_1 + r_2\omega_1 p_2}{\Lambda(\delta + \mu_h)}(\delta + 1), \qquad a_3 = a_2\Lambda + a_1\mu_h, \qquad a_4 = a_3 a + b\Lambda, \\ &a_5 = a + L_F b, \qquad a_6 = a + L_E b, \qquad a_7 = a_6\beta_F + a_5\beta_E, \qquad a_8 = (\beta_F L_E + \beta_E L_F)c, \\ &a_9 = (a_5 L_E + a_6 L_F)c \qquad \text{and} \qquad a_{10} = L_E L_F c^2. \end{aligned}$$

The coefficient c_4 of the polynomial equation (25) is always non-negative and c_0 is positive (negative) if $\mathcal{R}_0$ is less than (greater than) the unity, respectively. It is established in Appendix B that when $\mathcal{R}_0 > 1$, the coefficients c_1, c_2 and c_3 are negative. Then, using the Descartes Rules of Signs, we have established the following result.

Table 2
PRCC of model's parameters (Range variation at 10%).

	PRCCs and significance									
Parameters	Value	Range	S	I_1	I_2	R	F_V	F_B	E_V	E_B
Λ	28	[25.2 – 30.8]	0.8803**	0.6937**	0.6631**	0.6598**	0.5476**	0.4183*	0.5910	0.4431**
β_I	0.005	[0.0045 – 0.0055]	−0.2688	0.6937	0.2365	0.2956*	0.1745	0.41883	0.3356	0.2653
β_E	0.002	[0.0018 – 0.0022]	−0.1353	0.1935	−0.0968	−0.1234	0.0971	−0.0903	0.1603	0.1125
β_F	0.001	[0.0099 – 0.0011]	−0.9889**	0.0713**	0.9859**	0.9832**	0.9867**	0.9701**	0.9859**	0.9760**
p	0.2	[0.18 – 0.22]	0.1192	0.9878	0.0495	−0.5979**	0.1641	0.3047	−0.0341	−0.0878
δ	0.0092	[0.00828 – 0.01012]	0.0394	0.1327**	0.6248**	−0.0040	−0.0912	0.0726	0.0117**	−0.1857
μ_h	0.0104	[0.00936 – 0.01144]	−0.8240**	0.6041**	−0.7880**	−0.7796**	−0.6503**	−0.6748**	−0.7778	−0.6439**
d	0.046	[0.0414 – 0.0506]	0.1243	−0.7035	−0.2977*	0.0329	−0.1527	0.0397	0.0571	−0.0370
r_1	0.045	[0.0405 – 0.0495]	0.0269	−0.2694	−0.3407*	−0.0470	−0.0618	0.0492	−0.1669	−0.1778
r_2	0.0045	[0.00405 – 0.00495]	0.2967	0.0020	−0.0690	0.4106*	−0.0501	0.1000	−0.2711	0.0060
α_1	70	[63 – 77]	−0.0515	0.1223	0.0095	0.1375	−0.0299	−0.1155	0.0521	−0.1372
α_2	10	[9 – 11]	−0.2413	0.1057	0.4115*	0.1063	0.4178*	−0.5242**	0.6710**	0.5103**
μ_b	1.06	[1.166 – 0.954]	0.2856	−0.3243*	−0.2310	0.3129*	−0.5023**	−0.6204**	−0.5981**	−0.3899**
ϵ	0.7	[0.63 – 0.77]	−0.0265	−0.0561	−0.1823	0.0694	0.0058	−0.0542	−0.3708**	−0.3042**
η	0.05	[0.045 – 0.055]	−0.4620	0.0142	−0.0608	−0.2353	−0.1945	−0.1064	0.4895**	0.1999**
M_p	10^{10}	$[9.10^9 - 11.10^9]$	0.2193	−0.0834	−0.0948	−0.0831	−0.1258	−0.1146	−0.1313	−0.1571
K_f	10^4	$[9.10^3 - 11.10^3]$	0.5150**	−0.01886	−0.3617	−0.2497	−0.27561	−0.2324	−0.2212	−0.3234
K_e	10^6	$[9.10^5 - 11.10^5]$	−0.0408	−0.0114	0.0406	−0.0105	0.0291	−0.0820	−0.1877	0.1115*
Q_f	10^5	$[9.10^4 - 11.10^4]$	−0.0445	−0.1472	0.1098	0.1938	−0.1765	0.0907	−0.1261	0.0209
φ_v	0.05	[0.045 – 0.055]	0.1264	0.0806	0.0179	−0.0497	0.0146	−0.1073	0.0760	0.1398
φ_b	0.008	[0.0072 – 0.0088]	−0.0018	0.0605	0.0110	0.0056	−0.1079	0.4828**	0.0326	0.0272
θ_v	0.08	[0.072 – 0.088]	−0.0449	0.1800	−0.0066	0.1137	0.2243	−0.0831	0.0493	−0.3147
θ_b	0.005	[0.0045 – 0.0055]	−0.0769	0.1243	−0.1240	0.0298	−0.0396	0.0758	−0.0606	0.1721
g	0.73	[0.657 – 0.803]	0.0371	0.0190	−0.0167	−0.0931	−0.1565	−0.0368	0.1056	−0.1801

*: p-value <0.01,**: p-value <0.001

Proposition 1. *Model system (7) has exactly one endemic equilibrium whenever* $\mathcal{R}_0 > 1$.

In order to analyze the stability of the endemic equilibrium point of model system (7), we make use of the Centre Manifold theory [42] as described by Theorem 4.1 of Castillo-Chavez and Song [43] stated in Appendix C for convenience to establish the local asymptotic stability of the endemic equilibrium Q^* of model system (7).

The following result has been established.

Theorem 3. *The endemic equilibrium* Q^* *of model system (7) is locally asymptotically stable in* Ω *when* $\mathcal{R}_0 > 1$ *but close to 1.*

4. Numerical studies

In this section, we give numerical simulations that support the theory presented in the previous sections.

4.1. Sensitivity analysis of model's parameters

We carry out sensitivity analysis to ascertain the uncertainty of the parameters to the model output. This is vital since it enables us to identify critical input parameters that should be the center of focus if the disease is to be contained. Sensitivity and uncertainty analysis are performed using the Latin hypercube sampling (LHS) scheme, a Monte–Carlo stratified sampling method that allows us to obtain an unbiased estimate of the model output for a given set of input parameter values. The parameter space is simultaneously sampled without replacement and assuming statistical independence between the parameters. The selected sample is used to compute unbiased estimates of output values for state variables. We use a predefined variation of the model parameters at 10% and 50% relative to the referential values. Using algorithm from [44], we compute the partial ranking correlation coefficient (PRCC) of parameters against model's variables S, I_1, I_2, R, F_V, F_B, E_V, E_B. We use a fairly large sample of size $N = 1000$ to identify relationships between parameters and output variables. A positive (negative) correlation coefficient corresponds to an increasing (decreasing) monotonic trend between the model's variable and the parameter under consideration.

Note that, one parameter in Tables 2 and 3 is said "significantly correlate to one state variable" if absolute value of PRCC is more than 0.5 and p-value <0.001.

Table 4 presents the six most influential parameters of model system (7). According to the result obtained in Table 4, the parameters μ_h, β_F, μ_b, α_2, β_I and r_2 are the six most influential parameters of model system (7). This suggests that effective control strategy would be the implementation of intense awareness campaigns of the population on the risks of contact transmission which should be combined with a fast strategies of treatment and of isolation of infectious symptomatic.

Table 3
PRCC of model's parameters (Range variation at 50%).

	PRCCs and significance									
Parameters	Value	Range	S	I_1	I_2	R	F_V	F_B	E_V	E_B
Λ	28	[14 – 29.4]	0.9215**	0.4233**	0.3548*	0.3681**	0.3173*	0.3525*	0.3863**	0.2517
β_I	0.005	[0.0025 – 0.0075]	0.0826	0.9406**	0.8887**	0.9558**	0.8697**	0.8725**	0.8765**	0.9105**
β_E	0.002	[0.001 – 0.003]	−0.0804	0.3207*	0.2544	0.0424	0.0738	0.1712	0.1446	−0.1088
β_F	0.001	[0.0005 – 0.0015]	0.0028	0.4938**	0.5930**	0.6196**	0.2462	0.6131**	0.2672	0.4966**
p	0.2	[0.1 – 0.3]	−0.0897	−0.2107	−0.2580	−0.8732**	−0.2193	−0.0640	−0.0468	−0.0159
δ	0.0092	[0.0046 – 0.0138]	−0.0141	0.7355**	0.0774	−0.1115	−0.0920	−0.1193	0.0419	0.1303
μ_h	0.0104	[0.0052 – 0.0152]	−0.9628**	0.9801**	−0.9808**	−0.9910**	−0.9662**	−0.9670**	−0.9742**	−0.9747**
d	0.046	[0.0023 – 0.069]	0.0932	0.2739	−0.1921	−0.1270	−0.0995	−0.2957**	−0.2107	0.0233
r_1	0.045	[0.0225 – 0.999]	−0.0832	−0.5946**	0.0146	−0.0976	−0.1121	−0.0317	−0.0375	−0.0538
r_2	0.0045	[0.0023 – 0.0068]	0.2169	−0.8859**	−0.8761**	−0.7932**	−0.8601**	−0.8006**	−0.8183**	−0.8432**
α_1	70	[35 – 105]	0.0282	−0.0556	−0.0249	0.1119	0.0395	0.1792	−0.1018	−0.1228
α_2	10	[5 – 15]	−0.0958	0.4179**	0.4652**	0.5015**	0.7972**	0.7828**	0.8085**	0.8189**
μ_b	1.06	[0.53 – 1.59]	0.0122	−0.1853	−0.3066*	−0.4817**	−0.6259**	−0.8264**	−0.7240**	−0.6708**
ϵ	0.70	[0.35 – 1.05]	−0.1372	−0.3436*	−0.3108*	−0.3438	−0.0661	−0.0782	−0.7714**	−0.8614**
η	0.05	[0.025 – 0.075]	0.0991	−0.2597	−0.0425	−0.2707*	−0.4009**	−0.6689**	0.5781**	0.3653*
M_p	10^{10}	$[5.10^9 - 15.10^9]$	0.0871	0.1311	−0.0075	−0.1945	0.0501	−0.0033	0.1670	0.2016
K_f	10^4	$[5.10^3 - 15.10^3]$	0.1003	−0.6834**	−0.4120**	−0.4736	−0.3451*	−0.5114**	−0.4302**	−0.4844**
K_e	10^6	$[5.10^5 - 15.10^5]$	0.0217	−0.0623	0.0643	−0.2704**	−0.1310	−0.1799	−0.0786	0.0622
Q_f	10^5	$[5.10^4 - 15.10^4]$	0.0304	0.2013	0.0466	0.1384	−0.0885	0.6970	0.0422	0.0178
φ_v	0.05	[0.025 – 0.075]	−0.0353	0.2926*	0.0323	−0.1808	0.0889	−0.0491	−0.0606	0.1984
φ_b	0.008	[0.004 – 0.012]	0.1397	0.1711	−0.0136	−0.0275	0.0514	0.107**1	0.1886	0.3448*
θ_v	0.08	[0.04 – 0.12]	0.1623	−0.0232	−0.0076	0.2911	0.0886	−0.0290	0.0304	−0.3943**
θ_b	0.005	[0.0025 – 0.0075]	0.1112	−0.2210	−0.0086	0.0344	0.0936	−0.0995	−0.0044	0.6996**
g	0.73	[0.365 – 1.095]	0.1778	0.0299	−0.0296	0.2503	−0.0364	−0.2758	−0.0337	0.2175

*: p-value <0.01,**: p-value <0.001

Table 4
The six most influential parameters of model system (7).

	Number of state variables significantly correlate		
Parameters	Range 10%	Range 50%	Total
μ_h	7	8	15
β_F	7	5	12
μ_b	4	4	8
α_2	3	5	8
β_I	1	7	8
r_2	0	7	7

4.2. General dynamics

Numerical simulations using a set of reasonable parameter values in Table 1 are carried out for illustrative purpose and to support the analytical results.

The associated bifurcation diagram using the parameter values of Table 1 is depicted in Fig. 2. From this figure, it clearly appears that model system (7) exhibits a forward bifurcation, that is the disease-free equilibrium is stable if $\mathcal{R}_0 \leq 1$, while if $\mathcal{R}_0 > 1$, the disease-free equilibrium is unstable and there exists a unique endemic equilibrium which is stable.

Fig. 3 is an illustration of Theorem 2, showing the GAS of the disease-free equilibrium of model system (7) using various initial conditions when $\beta_I = 0.002$, $\beta_F = 0.002$ and $\beta_E = 0.001$ (so that $\mathcal{R}_0 = 0.4552 < 1$). All other parameter values are as in Table 1. It illustrates that the disease disappears in the host population when $\mathcal{R}_0 \leq 1$.

Fig. 4 shows the stability of the endemic equilibrium Q^* of model system (7) as demonstrated in Theorem 3 when $\beta_I = 0.02$, $\beta_F = 0.02$ and $\beta_E = 0.01$ (so that $\mathcal{R}_0 = 3.9034 > 1$). All other parameter values are as in Table 1. Although the stability of the endemic equilibrium have been established analytically in a neighborhood of $\mathcal{R}_0 = 1$, numerical simulations show that the endemic equilibrium is stable over a wide range of values of $\mathcal{R}_0 > 1$.

Now, numerical simulations are carried out to investigate the impact of varying the proportion of symptomatic infected individuals, the effect of the virulence of bacteria and the role of the population of phytoplankton and zooplankton on the dynamical transmission of cholera within a human community. In all simulations, the transmission rates are chosen to be $\beta_I = 0.02$, $\beta_E = 0.01$ and $\beta_F = 0.02$ (so that $\mathcal{R}_0 > 1$). All other parameter values are as in Table 1. In all simulations, model system (7) was simulated with the following initial conditions which have been chosen arbitrarily: $S(0) = 1000$, $I_1(0) = 10$, $I_2(0) = 50$, $R(0) = 30$, $F_V(0) = 50,000$, $F_B(0) = 10,000$, $E_V(0) = 50,000$ and $E_B(0) = 10,000$. The "Total of infected human

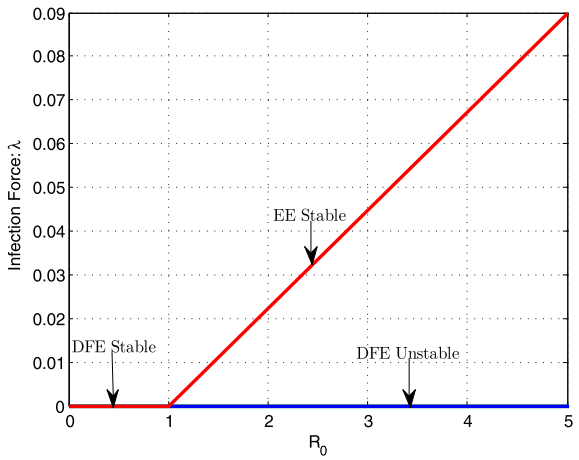

Fig. 2. Bifurcation diagram of model system (7). The notations DFE and EE stand for disease-free equilibrium and endemic equilibrium, respectively.

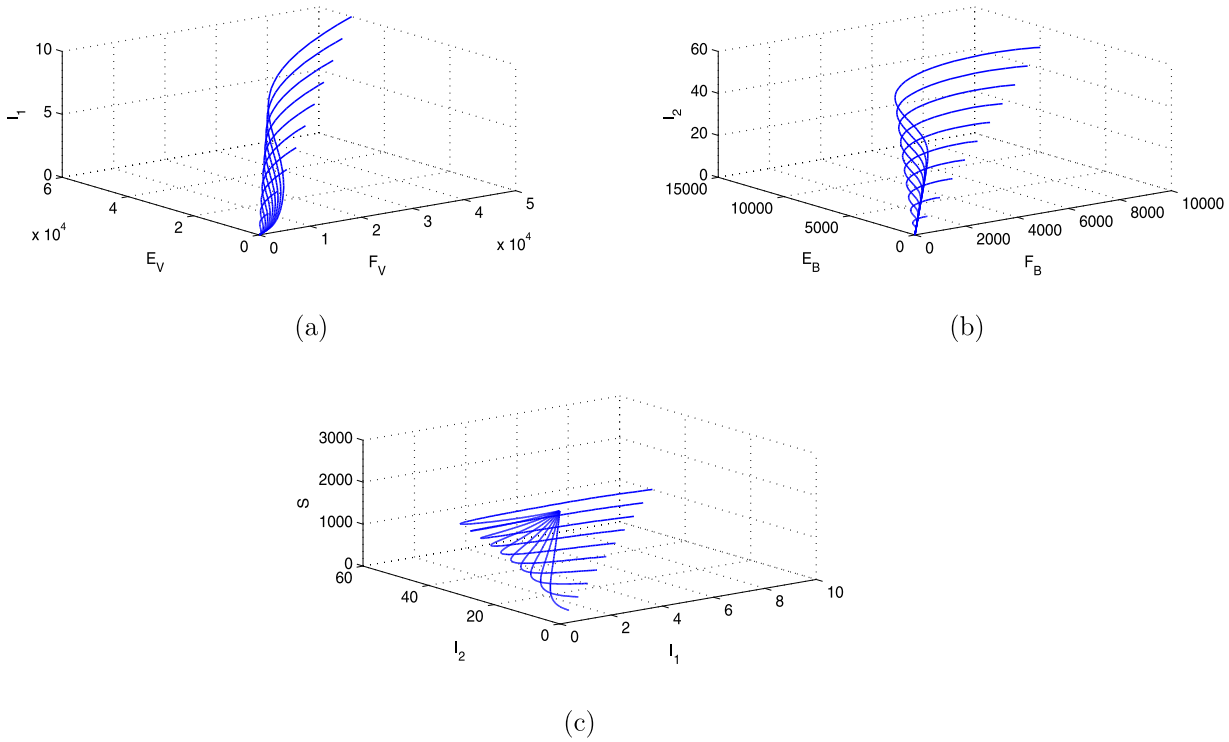

Fig. 3. GAS of the disease-free equilibrium Q_0 (Theorem 2).

population" is a cumulative value of I_1 and I_2. The "Total concentration of bacteria" is also a cumulative value of F_V, F_B, E_B and E_V. Results of numerical simulations are depicted in Figs. 5 and 6.

Case 1: Most people infected with cholera (80%) are asymptomatic and appear healthy although they carry the bacteria for two or three weeks and excrete them in wastewater. Since they carry bacteria for a long time than symptomatic infected without knowing, they can infect people around them. They contributes more to the spread of the disease [2,25]. Symptomatic infected can live with the disease for five day maximal.

To study the impact of the proportion of asymptomatic infected individuals on the outbreak of the infection, model system (7) was simulated for three different values of $1-p$: $1-p=0.9$ (so that $\mathcal{R}_0=4.1581$), $1-p=0.8$ (so that $\mathcal{R}_0=3.9034$) and $1-p=0.5$ (so that $\mathcal{R}_0=3.1392$). From Fig. 5(a), it is evident that as p increases (i.e. $1-p$ decreases), the total number of infected individuals decreases. This means that the presence of asymptomatic infected individuals within a human population contributes considerably to the spread of the disease. Since asymptomatic infected individuals are healthy carriers, it's difficult to identify them within a heterogeneous population for a possible

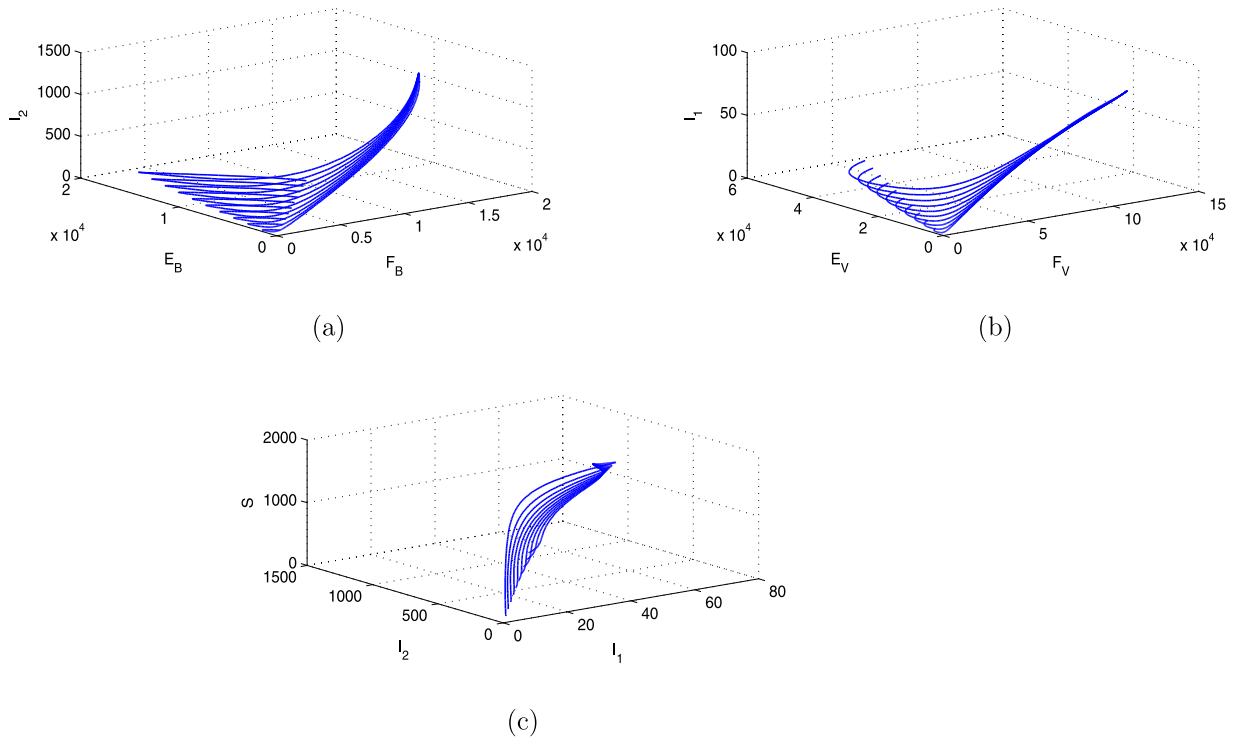

Fig. 4. Stability of the endemic equilibrium Q^* (Theorem 3).

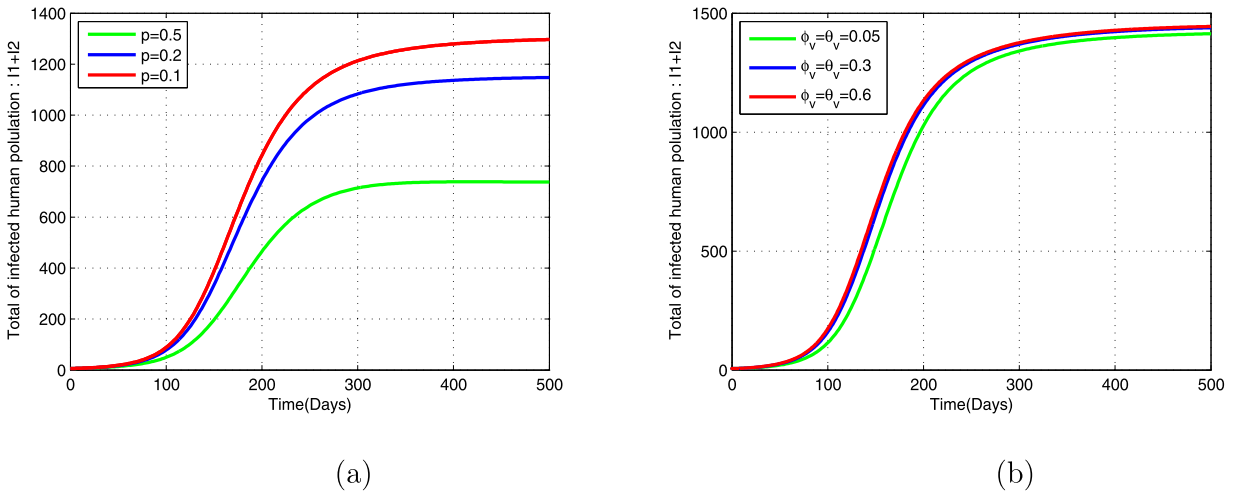

Fig. 5. Time series of the total number of infected individuals for three different values (a) the proportion of symptomatic infected individual η and (b) the virulence of bacteria $\theta_\nu = \varphi_\nu$.

treatment or isolation. Hence, it is urgent to educate the public on hygiene rules to avoid the intersection of the food chain with excrement chain.

Case 2: Here, we are interested to the case when the bacteria become more virulent. Without loss of generality, we assume that θ_ν and φ_ν have the same value, that is $\theta_\nu = \varphi_\nu$. Model system (7) was simulated for three different values of $\theta_\nu = \varphi_\nu$: $\theta_\nu = \varphi_\nu = 0.05$ (so that $\mathcal{R}_0 = 4.1581$), $\theta_\nu = \varphi_\nu = 0.3$ (so that $\mathcal{R}_0 = 4.4042$) and $\theta_\nu = \varphi_\nu = 0.6$ (so that $\mathcal{R}_0 = 4.5268$). From Fig. 5(b), the effect of virulence bacteria on infected people seems to be limited from $\theta_\nu = \varphi_\nu = 0.3$. This is du to the contacts between infected people and bacteria. Thus, even if bacteria are too virulent contact with human, adequate contacts between human and bacteria are necessary to trigger or favorise an cholera epidemic.

Case 3: According to biological review, the environmental reservoirs of *V. cholerae* promote the growth of the bacteria in the aquatic environment [45–48]. Fig. 6(a) shows the effect of varying the carrying capacity of the population of

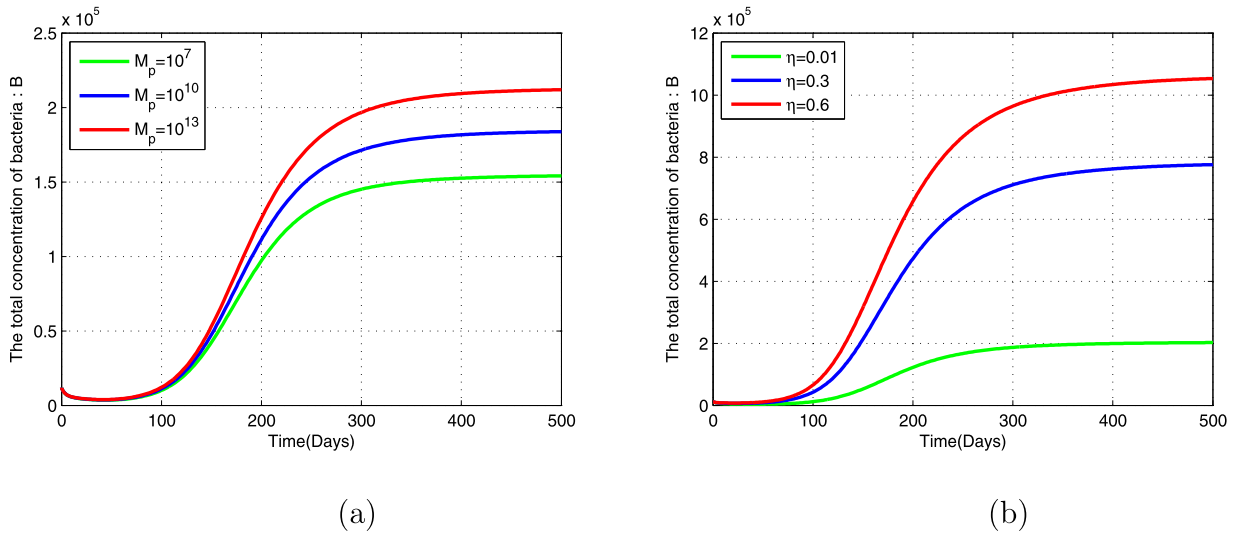

Fig. 6. Time series of the total concentration of bacteria for three different values of (a) the carrying capacity of aquatic reservoirs M_p and (b) the proportion of environmental bacteria that survives after their association with aquatic reservoirs η.

phytoplankton and zooplankton on the dynamics of bacteria. The simulation was performed for three different values of the carrying capacity of the population of phytoplankton and zooplankton M_p: $M_p = 10^7$ (so that $\mathcal{R}_0 = 3.7848$), $M_p = 10^{10}$ (so that $\mathcal{R}_0 = 3.9034$) and $M_p = 10^{13}$ (so that $\mathcal{R}_0 = 4.0183$). It clearly appears that as M_p increases, the concentration of the total bacteria increases. This is why, it is recommended to clean or destroy the potential risk areas where these reservoirs are growing. This will result on the reduction of the value of M_p.

Case 4: Simulation results in Fig. 6(b) illustrate the impact of varying the proportion of environmental bacteria that survives after their association with aquatic reservoirs on the dynamics of bacteria for three different values of η: $\eta = 0.01$ (so that $\mathcal{R}_0 = 4.1581$), $\eta = 0.3$ (so that $\mathcal{R}_0 = 5.1322$) and $\eta = 0.6$ (so that $\mathcal{R}_0 = 6.6087$). As expected by the result obtained in [49], it confirms the critical role of the reservoirs on the endemicity of cholera. Thus, the commensal association between bacteria and reservoirs may play an important role in the outbreak of cholera epidemic by favoring persistence of the pathogen during inter-epidemic periods.

4.3. Impact of environmental factors

Many studies in the literature supported that the bacteria associated with the zooplankton showed seasonal abundance, with the largest numbers occurring in the early spring and again in the summer, when zooplankton total numbers were correspondingly large [5–7,13–16]. Approximately 0.01–40% of the total water column bacteria were associated with zooplankton, with the percentage of the total water column bacteria population associated with zooplankton varying by season. Indeed, the variation of environmental factors may explain the seasonality of the disease either by exerting a direct influence on the bacterial reservoirs capacity (M_p) or even on their metabolism (φ_v, φ_b, θ_v, θ_b) [46]. Thus, the parameters φ_v, φ_b, θ_v, θ_b and M_p of model system (7) are assumed to be time-dependent parameters.

The virulent bacteria proportion in term of temperature (T) can be modeled as:

$$\varphi_v = \left(1 + e^{-(0.61\times T - 17.25)}\right)^{-1}. \tag{26}$$

Also, the parameter θ_v can be modeled as follows:

$$\theta_v = \varphi_v + (1-\varphi_v)\left(1 - e^{k\varepsilon}\right), \quad \text{with } k > 0, \tag{27}$$

where ε measures the capacity of environmental bacteria to face unfavorable conditions. If a living bacteria is not virulent it is assumed to be "viable but non-culturable" so that we have

$$\varphi_b = 1 - \varphi_v \ \text{ and } \theta_b = 1 - \theta_v. \tag{28}$$

The carrying capacity M_p of *V. cholerae* in the environment is assumed to be the following periodic function:

$$M_p(t) = M_{mean}\left(1 + \tilde{k}\sin(\frac{2\pi}{P}t)\right). \tag{29}$$

Note that M_p is a periodic function with the period $P = 365$ days. Without loss of generality, we choose $M_{mean} = 10^6$ and $\tilde{k} = 0.99$.

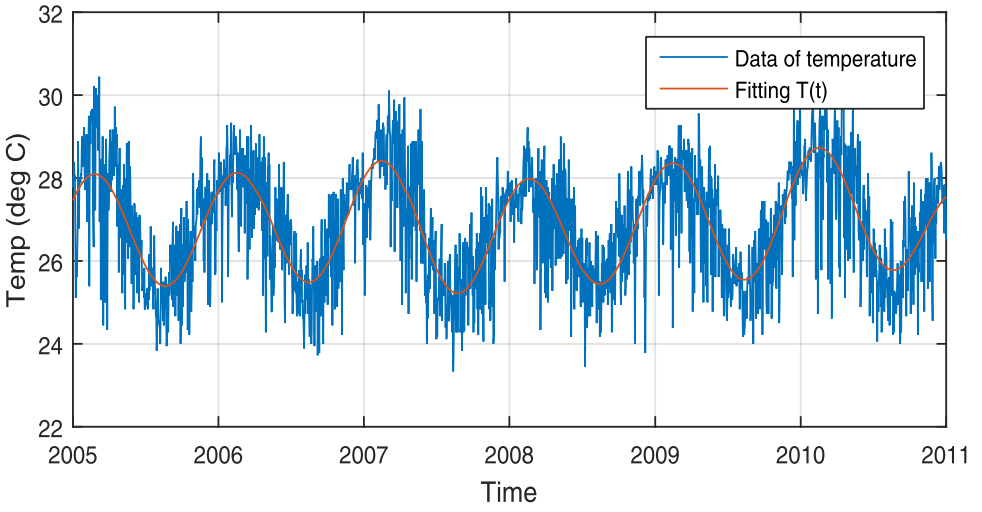

Fig. 7. Temperatures in Douala during 2005–2011 (Source: Postdam Institute of Climatology (PIK)).

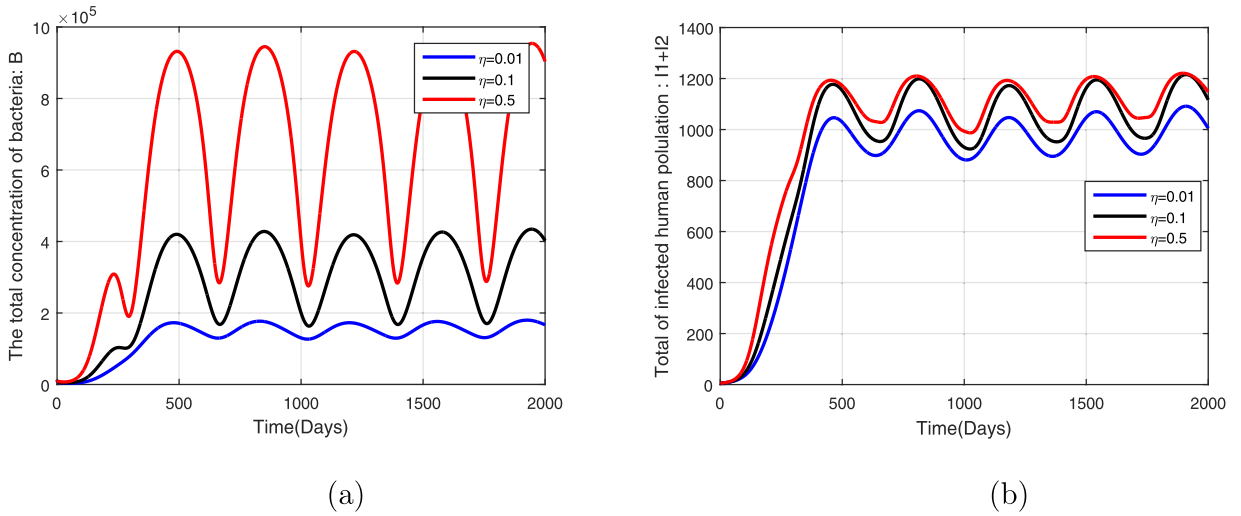

Fig. 8. Simulations of model system (7) showing the effect of varying of the commensalism force η on (a) bacteria density and (b) infected population.

The real data and the fitted curve of temperature in Douala (Cameroon) during period going from 2005 to 2011 are shown in Fig. 7. We use the cftool in Matlab R2015a to fit the statistical data of temperature and we obtain

$$\begin{aligned} T(t) = {} & 82.27\sin(0.0009097x + 0.7393) + 55.7\sin(0.001133x + 3.683) \\ & + 0.3052\sin(0.003942x + 5.162) + 1.42\sin(0.01734x + 0.7017) \\ & + 0.1663\sin(0.01001x + 0.4355) \end{aligned} \tag{30}$$

Now, we derive some simulations in order to evaluate the both impact of metabolic change and density reservoirs in bacteria and infected population. Model system (7) is simulated with the time-dependent parameters φ_v, φ_b, θ_v, θ_b and M_p.

Fig. 8 is obtained for three different values of η which represents the commensalism intensity between bacteria et reservoirs. From Fig. 8(a), it clearly appears that this association play an important role on the persistence of bacteria in environment. Also, from Fig. 8(b), one can observe that the commensalism force η does not impacts evenly the number of infected people. This implies that cholera epidemic can be limited or avoided even if the associated reservoirs of bacteria are exponentially growing.

Fig. 9 presents the result of numerical simulations of model system (7) for three different values of the mean number of bacteria reservoirs M_{mean}. It illustrates the growth of bacteria is also exponential when M_{mean} grow, but that of infected is relatively moderate like previously.

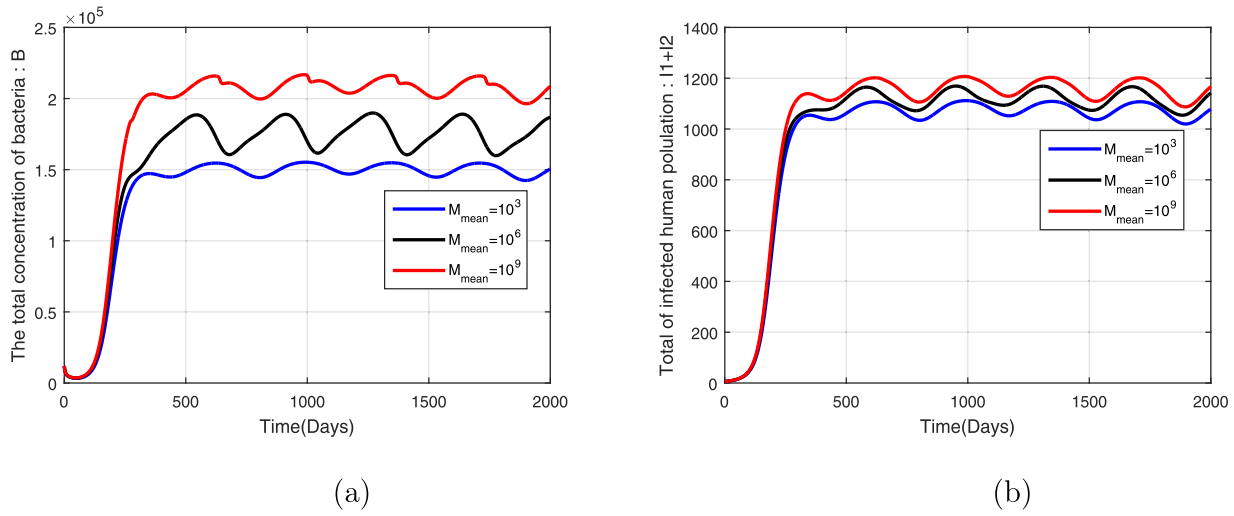

Fig. 9. Simulations of model system (7) showing the effect of mean reservoirs capacity M_{mean} on (a) bacteria density and (b) infected population.

5. Conclusion

In this paper, we have proposed and analyzed a deterministic model for the dynamical transmission of cholera within a human community. The considered model takes into account the change of metabolism of bacteria and the commensal relationship of bacteria with the environmental reservoirs on the persistence of the disease. Indeed, in many cholera models in the literature, these biological facts have been neglected through unrealistic assumptions such as *V. cholerae* are always virulent [16] and at birth, *V. cholerae* are hyperinfectious, lose their virulence after certain time and remains non hyper infection until the end of their live [19,20].

In this work, we have considered a mathematical model for the dynamical transmission of cholera in which the following biological and epidemiological facts are incorporated: (i) the waning of recovery-induced of immunity of recovered individuals (ii) the virulence of bacteria and (iii) the commensal relationship between bacteria and the population of phytoplankton and zooplankton. The objective was to investigate the impact of environmental factors on the dynamical transmission of cholera within a human population. A qualitative analysis of the model has been presented. Our findings on the long term dynamics of the system can be summarized as follows.

1. We computed the disease-free equilibrium and derived the basic reproduction number $\mathcal{R}_0$ that determines the outcome of the disease.
2. We proved that the disease-free equilibrium is globally asymptotically stable whenever $\mathcal{R}_0 \leq 1$ on a positively invariant region.
3. We showed that the model has a unique endemic equilibrium when $\mathcal{R}_0 > 1$. We also established the local asymptotic stability of the unique endemic equilibrium when $\mathcal{R}_0 > 1$ but close to 1.
4. The sensitivity analysis of the system has been performed. We found that in an epidemic situation it is urgent to sensibilize population about the risk of transmission through contact and to take on charge rapidly the infected people by isolating them from susceptible
5. Numerical results have been presented to illustrate and validate theoretical results. Though numerical simulation, we found that the aquatic reservoirs are playing a significant role among the factors explaining the causes of endemicity of these disease.

Different improvements and extensions of the model on which we are still working include: introducing of time-dependent parameters in order to integrate fluctuation of environmental factors du to periodic variations of climate, control strategies and extension to 2 patches.

Acknowledgments

The authors acknowledge with gratitude the support from the Saint Jerome Catholic University Institute of Douala-Cameroon and LMAH of University of Havre in France.

Appendix A. Proof of $\rho(\overline{A_2}) \leq 0 \Leftrightarrow \mathcal{R}_0 \leq 1$

Herein, we show that the condition $\rho(\overline{A_2}) \leq 0$ is equivalent to $\mathcal{R}_0 \leq 1$.

To check condition ($\boldsymbol{H_5}$) of theorem from Kamgang and Sallet [50], we will use the following lemma:

Lemma 3. *: Let M be a square Metzler matrix written in block form $M = \begin{bmatrix} \mathcal{A} & \mathcal{B} \\ \mathcal{C} & \mathcal{D} \end{bmatrix}$ where $\mathcal{A}$ and $\mathcal{D}$ are square matrices. Then, the matrix M is Metzler stable if and only if matrices $\mathcal{A}$ and $\mathcal{D} - \mathcal{C}\mathcal{A}^{-1}\mathcal{B}$ (or $\mathcal{D}$ and $\mathcal{A} - \mathcal{B}\mathcal{D}^{-1}\mathcal{C}$) are Metzler stable.*

The matrix $\bar{A}_2$ can be expressed in the form of the matrix M with

$$\mathcal{A} = \begin{bmatrix} -\omega_1 + p_1\beta_I & p_1\beta_I \\ p_2\beta_I & -\omega_2 + p_2\beta_I \end{bmatrix}, \qquad \mathcal{B} = \begin{bmatrix} \frac{p_1\beta_F S_0}{K_F} & 0 & \frac{p_1\beta_E S_0}{K_E} & 0 \\ \frac{p_2\beta_F S_0}{K_F} & 0 & \frac{p_2\beta_E S_0}{K_E} & 0 \end{bmatrix},$$

$$\mathcal{C} = \begin{bmatrix} \alpha_1 & \alpha_2 \\ 0 & 0 \\ 0 & 0 \\ 0 & 0 \end{bmatrix} \quad \text{and} \quad \mathcal{D} = \begin{bmatrix} -M_b & \varphi_v & 0 & 0 \\ \varphi_b & -M_v & 0 & 0 \\ \Sigma_\eta & 0 & -N_b & \theta_v \\ 0 & \Sigma_\eta & \theta_b & -N_v \end{bmatrix}.$$

The matrix $\mathcal{A}$ is Metzler stable if and only if $\beta_I < \frac{\omega_1\omega_2}{\omega_2 p_1 + \omega_1 p_2}$. A simple calculation yields

$$\mathcal{A} - \mathcal{B}\mathcal{D}^{-1}\mathcal{C} = \begin{bmatrix} -(\omega_1 - p_1\beta_I) + \mathcal{R}_{01F} + \mathcal{R}_{01E} & p_1\beta_I + (\mathcal{R}_{02F} + \mathcal{R}_{02E})\frac{p_1}{p_2} \\ p_2\beta_I + (\mathcal{R}_{01F} + \mathcal{R}_{01E})\frac{p_2}{p_1} & -(\omega_2 - p_2\beta_I) + \mathcal{R}_{02F} + \mathcal{R}_{02E} \end{bmatrix},$$

where

$$\begin{aligned} \mathcal{R}_{0iF} &= \beta_F \frac{p_i\alpha_i S_0\big(\varphi_v + \Sigma_\eta + D_1\big)}{\omega_i K_F\big(\Sigma_\eta + D_1\big)\big(\Sigma_\eta + D_1 + \varphi_b + \varphi_v\big)}, \\ \mathcal{R}_{0iE} &= \beta_E \frac{p_i\alpha_i S_0\Sigma_\eta\big[\big(\varphi_v + \Sigma_\eta + D_1\big)(\theta_v + D_2) + \varphi_b\theta_v\big]}{\omega_i K_E D_2(D_2 + \theta_b + \theta_v)\big(\Sigma_\eta + D_1\big)\big(\Sigma_\eta + D_1 + \varphi_b + \varphi_v\big)}, \end{aligned} \tag{31}$$

for $i \in \{1, 2\}$. Then, it is easy to verify that the matrices $\mathcal{A}$ and $\mathcal{A} - \mathcal{B}\mathcal{D}^{-1}\mathcal{C}$ are Metzler stable if and only if $\mathcal{R}_0 \le 1$.

Appendix B. Proof of the non positivity of coefficients of the polynomial equation (25) when $\mathcal{R}_0 > 1$

Herein, we show that the coefficients c_1, c_2 and c_3 of the polynomial (25) are all negative whenever $\mathcal{R}_0 > 1$.
Let

$$\mathcal{R}_{0E} = \mathcal{R}_{01E} + \mathcal{R}_{02E}, \qquad \mathcal{R}_{0F} = \mathcal{R}_{01F} + \mathcal{R}_{02F}, \qquad \mathcal{R}_{0I} = \beta_1\Big(\frac{p_1}{\omega_1} + \frac{p_2}{\omega_2}\Big) \qquad \text{and}$$
$$\chi = \frac{\mu_h}{\omega_2}[\delta\omega_1((1-r_2)\omega_1 p_2 + (1-r_1)\omega_2 p_1) + (\omega_2 p_1 + \omega_1 p_2)\Lambda\mu_h] + (r_1\omega_2 p_1 + r_2\omega_1 p_2)p_1\Lambda(\delta+1).$$

With the above notations, the coefficients c_0, c_1, c_2, c_3 and c_4 of the polynomial equation (25) become

$$\begin{cases} c_0 &= \Lambda L_E L_F c^3(1 - \mathcal{R}_0), \\ c_1 &= \Lambda c^2[a_5 L_E(1 - R_{0I} - R_{0E}) + a_6 L_F(1 - R_{0I} - R_{0F})] \\ &\quad + L_E L_F c^2[\chi(1 - R_{0F} - R_{0E}) + S_0 c(1 - R_0)], \\ c_2 &= aa_1 L_E L_F c^3(1 - R_{0F} - R_{0E}) + \chi c[a_5 L_E(1 - R_{0E}) + a_6 L_F(1 - R_{0F})] \\ &\quad + S_0 c^2(1 - R_{0I})[L_E a_5(1 - R_{0E}) + L_F a_6(1 - R_{0F})], \\ c_3 &= a_5 a_6 \chi + a_5 a_6 S_0 c(1 - R_{0I}) + aa_1 c[L_E a_5(1 - R_{0E}) + L_F a_6(1 - R_{0F})], \\ c_4 &= aa_1 a_5 a_6. \end{cases} \tag{32}$$

Then, it clearly appears that $c_i > 0$, $i \in \{1, 2, 3, 4\}$ when $\mathcal{R}_0 \le 1$. Therefore, when $\mathcal{R}_0 > 1$, the coefficients c_i, $i \in \{1, 2, 3, 4\}$ are all negative. Consequently, the polynomial equation (25) has exactly one real positive solution when $\mathcal{R}_0 > 1$.

Appendix C. Proof of Theorem 3

In this Appendix, we give the proof of Theorem 3 on the local stability of the endemic equilibrium point of system (7). To do so, the following simplification and change of variables are made first to all. Let $x_1 = S$, $x_2 = I_1$, $x_3 = I_2$, $x_4 = R$, $x_5 = F_V$, $x_6 = F_B$, $x_7 = E_V$ and $x_8 = P$ so that $N = x_1 + x_2 + x_3 + x_4$. Further, by using the vector notation $x = (x_1, x_2, x_3, x_4, x_5, x_6, x_7, x_8)^T$, model system (7) can be written in the form $\dot{x} = f(x)$ with $f = (f_1, f_2, f_3, f_4, f_5, f_6, f_7, f_8)^T$ as

follows:

$$\begin{cases} \dot{x_1} = \Lambda + \delta x_4 - (\lambda + \mu_h)x_1, \\ \dot{x_2} = p_1\lambda x_1 - \omega_1 x_2, \\ \dot{x_3} = p_2\lambda x_1 - \omega_2 x_3, \\ \dot{x_4} = r_1 x_2 + r_2 x_3 - (\delta + \mu_h)x_4, \\ \dot{x_5} = \alpha_1 x_2 + \alpha_2 x_3 + \varphi_v x_6 - M_b F_V, \\ \dot{x_6} = \varphi_b x_5 - M_v x_6, \\ \dot{x_7} = \Sigma_\eta x_5 + \theta_v x_8 - N_b x_7, \\ \dot{x_8} = \Sigma_\eta x_6 + \theta_b x_7 - N_v x_8, \end{cases} \tag{33}$$

where $\lambda = \beta_F \frac{x_5}{x_5+K_f} + \beta_E \frac{x_7}{x_7+K_e} + \beta_I \frac{x_2+x_3}{x_1+x_2+x_3+x_4}$. System (33) has a DFE given by $Q_0 = (S_0, 0, 0, 0, 0, 0, 0, 0)$ where $S_0 = \frac{\Lambda}{\mu_h}$. The Jacobian of system (33) at the DFE Q_0 is

$$J(Q_0) = \begin{bmatrix} -\mu_h & -\beta_I & -\beta_I & \delta & -\beta_F\frac{S_0}{K_F} & 0 & -\beta_E\frac{S_0}{K_E} & 0 \\ 0 & -(\omega_1 - p_1\beta_I) & p_1\beta_I & 0 & p_1\beta_F\frac{S_0}{K_F} & 0 & p_1\beta_E\frac{S_0}{K_E} & 0 \\ 0 & p_2\beta_I & -(\omega_2 - p_2\beta_I) & 0 & p_2\beta_F\frac{S_0}{K_F} & 0 & p_2\beta_E\frac{S_0}{K_E} & 0 \\ 0 & r_1 & r_2 & -(\delta+\mu_h) & 0 & 0 & 0 & 0 \\ 0 & \alpha_1 & \alpha_2 & 0 & -M_b & \varphi_v & 0 & 0 \\ 0 & 0 & 0 & 0 & \varphi_b & -M_v & 0 & 0 \\ 0 & 0 & 0 & 0 & \Sigma_\eta & 0 & -N_b & \theta_v \\ 0 & 0 & 0 & 0 & 0 & \Sigma_\eta & \theta_b & -N_v \end{bmatrix}.$$

The basic reproduction number of the transformed (linearized) model system (33) is the same as that of the original model given by Eq. (7). Therefore, choosing β_I as a bifurcation parameter by solving for β_I when $\mathcal{R}_0 = 1$, one obtains

$$\beta_I = \beta_I^* = \left[1 - \left(\frac{\beta_F S_0(\varphi_v+\Sigma_\eta+D_1)}{K_F(\Sigma_\eta+D_1)(\Sigma_\eta+D_1+\varphi_b+\varphi_v)} + \frac{\beta_E S_0 \Sigma_\eta\left[(\varphi_v+\Sigma_\eta+D_1)(\theta_v+D_2)+\varphi_b\theta_v\right]}{K_E D_2(D_2+\theta_b+\theta_v)(\Sigma_\eta+D_1)(\Sigma_\eta+D_1+\varphi_b+\varphi_v)}\right)\sum_{i=1}^{2}\frac{p_i\alpha_i}{\omega_i}\right]\frac{\omega_1\omega_2}{p_1\omega_2+p_2\omega_1}. \tag{34}$$

It follows that the Jacobian $J(Q_0)$ of system (33) at the DFE Q_0, with $\beta_I = \beta_I^*$, denoted by J_{θ^*} has a simple zero eigenvalue (with all other eigenvalues having negative real parts). Hence, the Centre Manifold theory [43] can be used to analyze the dynamics of system (33). In particular, the theorem in Castillo and Song [37], reproduced below for convenience, will be used to show that when $\mathcal{R}_0 > 1$ there exists an endemic equilibrium of system (33) which is locally asymptotically stable for $\mathcal{R}_0$ near 1 under certain conditions.

Theorem 4 (Castillo-Chavez and Song [42]). *Consider the following general system of ordinary differential equations with a parameter Φ:*

$$\frac{dz}{dt} = f(x, \Phi)\ , f : \mathbb{R}^n \times \mathbb{R} \text{ and } f \in C^2(\mathbb{R}^n, \mathbb{R}), \tag{35}$$

where 0 is an equilibrium point of the system (that is, $f(0, \Phi) \equiv 0$ for all Φ) and assume

1. $A = D_z f(0,0) = \left(\frac{\partial f_i}{\partial z_j}(0,0)\right)$ is the linearization matrix of system (35) around the equilibrium 0 with Φ evaluated at 0. Zero is a simple eigenvalue of A and other eigenvalues of A have negative real parts;

2. Matrix A has a right eigenvector u and a left eigenvector v (each corresponding to the zero eigenvalue). Let f_k be the k^{th} component of f and

$$a = \sum_{k,i,j=1}^{n} v_k u_i u_j \frac{\partial^2 f_k}{\partial x_i \partial x_j}(0,0) \text{ and } b = \sum_{k,i=1}^{n} v_k u_i \frac{\partial^2 f_k}{\partial x_i \partial \Phi}(0,0),$$

then, the local dynamics of the system around the equilibrium point 0 is totally determined by the signs of a and b.

1. *$a > 0$, $b > 0$. When $\Phi < 0$ with $|\Phi| \ll 1$, 0 is locally asymptotically stable and there exists a positive unstable equilibrium; when $0 < \Phi \ll 1$, 0 is unstable and there exists a negative, locally asymptotically stable equilibrium;*
2. *$a < 0$, $b < 0$. When $\Phi < 0$ with $|\Phi| \ll 1$, 0 is unstable; when $0 < \Phi \ll 1$, 0, is locally asymptotically stable equilibrium, and there exists a positive unstable equilibrium;*
3. *$a > 0$, $b < 0$. When $\Phi < 0$ with $|\Phi| \ll 1$, 0 is unstable and there exists a locally asymptotically stable negative equilibrium; when $0 < \Phi \ll 1$, 0 is stable, and a positive unstable equilibrium appears;*
4. *$a < 0$, $b > 0$. When Φ changes from negative to positive, 0 changes its stability from stable to unstable. Correspondingly a negative unstable equilibrium becomes positive and locally asymptotically stable.*

In order to apply the above theorem, the following computations are necessary (it should be noted that we are used β_I^* as the bifurcation parameter, in place of Φ in Theorem 4).

Eigenvectors of $J_{\beta_I^*}$: For the case when $\mathcal{R}_0 = 1$, it can be shown that the Jacobian of system (33) has a right eigenvector (corresponding to the zero eigenvalue), given by $U = (u_1, u_2, u_3, u_4, u_5, u_6, u_7, u_8)^T$, where

$$u_1 = -\zeta_1 u_2, \qquad u_2 = u_2 > 0, \qquad u_3 = \zeta_3 u_2, \qquad u_4 = \zeta_4 u_2, \qquad u_5 = \zeta_5 u_2,$$

$$u_6 = \zeta_6 u_2, \qquad u_7 = \zeta_7 u_2 \qquad \text{and} \qquad u_8 = \zeta_8 u_2,$$

where

$$\zeta_1 = \frac{1}{\mu_h}\left[1 - \frac{\delta r_1}{\delta+\mu_h} + \frac{p_2\omega_1}{p_1\omega_2}\left(1 - \frac{\delta r_2}{\delta+\mu_h}\right) + S_0\left(\frac{\beta_F}{K_F}\zeta_5 + \frac{\beta_E}{K_E}\zeta_7\right)\right], \qquad \zeta_3 = \frac{p_2\omega_1}{p_1\omega_2},$$

$$\zeta_4 = \frac{r_1 p_1\omega_2 + r_2 p_2\omega_1}{p_1\omega_2(\delta+\mu_h)}, \qquad \zeta_5 = \frac{\left(\varphi_v + \Sigma_\eta + D_1\right)(\alpha_1 p_1\omega_2 + \alpha_2 p_2\omega_1)}{p_1\omega_2\left(\Sigma_\eta + D_1\right)\left(\Sigma_\eta + D_1 + \varphi_b + \varphi_v\right)}, \quad \zeta_6 = \frac{\varphi_b}{\varphi_v + \Sigma_\eta + D_1}\zeta_5,$$

$$\zeta_7 = \frac{\Sigma_\eta\left((\varphi_v + \Sigma_\eta + D_1)(\theta_v + D_2) + \theta_v\varphi_b\right)}{\left(\varphi_v + \Sigma_\eta + D_1\right)D_2(D_2 + \theta_b + \theta_v)}\zeta_5 \quad \text{and} \quad \zeta_8 = \frac{\theta_b(\varphi_v + \Sigma_\eta + D_1) + (\theta_b + D_2)\varphi_b}{\left((\varphi_v + \Sigma_\eta + D_1)(\theta_v + D_2) + \theta_v\varphi_b\right)}\zeta_7.$$

Similarly, the components of the left eigenvectors of $J_{\beta_I^*}$ (corresponding to the zero eigenvalue), denoted by $V = (v_1, v_2, v_3, v_4, v_5, v_6, v_7, v_8)^T$, are given by

$$v_1 = 0, \quad v_2 = v_2 > 0, \quad v_3 = \Gamma_3 v_2, \quad v_4 = 0, \quad v_5 = \Gamma_5 v_2, \quad v_6 = \Gamma_6 v_2, \quad v_7 = \Gamma_7 v_2 \text{ and } v_8 = \Gamma_8 v_2,$$

where

$$\Gamma_3 = \frac{p_1\beta_I^*\alpha_1 + \alpha_2\left(\omega_1 - p_1\beta_I^*\right)}{p_2\beta_I^*\alpha_2 + \alpha_1\left(\omega_2 - p_2\beta_I^*\right)},$$

$$\Gamma_5 = \frac{\left(\varphi_v + \Sigma_\eta + D_1\right)\beta_F S_0(p_1 + p_2\Gamma_3) + \Sigma_\eta\left(\left(\varphi_v + \Sigma_\eta + D_1\right)\Gamma_7 + \varphi_v\Gamma_8\right)}{K_F\left(\Sigma_\eta + D_1\right)\left(\Sigma_\eta + D_1 + \varphi_b + \varphi_v\right)}$$

$$\Gamma_6 = \frac{\varphi_v\beta_E S_0(p_1 + p_2\Gamma_3) + \Sigma_\eta\left(\left(\varphi_b + \Sigma_\eta + D_1\right)\Gamma_8 + \varphi_v\Gamma_7\right)}{K_E\left(\Sigma_\eta + D_1\right)\left(\Sigma_\eta + D_1 + \varphi_b + \varphi_v\right)},$$

$$\Gamma_7 = \frac{(\theta_v + D_2)\beta_E S_0(p_1 + p_2\Gamma_3)}{K_E D_2(D_2 + \theta_b + \theta_v)} \qquad \text{and} \qquad \Gamma_8 = \frac{\theta_v}{\theta_v + D_2}\Gamma_7$$

Using Eq. (34) we can easily deduce that $\omega_1 - p_1\beta_I^* > 0$ and $\omega_2 - p_2\beta_I^* > 0$, this ensures the fact that $\Gamma_3 > 0$

Computation of b: For the sign of b, it can be shown that the associated non-vanishing partial derivatives of f are

$$\frac{\partial^2 f_1}{\partial x_2\partial\beta^*_I} = -1, \frac{\partial^2 f_1}{\partial x_3\partial\beta_I^*} = -1, \frac{\partial^2 f_2}{\partial x_2\partial\beta^*_I} = p_1, \quad \frac{\partial^2 f_2}{\partial x_3\partial\beta^*_I} = p_1,$$
$$\frac{\partial^2 f_3}{\partial x_2\partial\beta^*_I} = p_2 \quad \text{and} \quad \frac{\partial^2 f_3}{\partial x_3\partial\beta_I} = p_2.$$

It follows that

$$\begin{aligned} b &= v_2\textstyle\sum_{i=1}^{8} u_i\frac{\partial^2 f_2}{\partial x_i\partial\beta_I^*} + v_3\sum_{i=1}^{8} u_i\frac{\partial^2 f_3}{\partial x_i\partial\beta_I^*}, \\ &= u_2 v_2\left(1 + \frac{p_2\omega_1}{p_1\omega_2}\right)(p_1 + \Gamma_3 p_2) > 0. \end{aligned}$$

Computation of a: For system (33), the associated non-zero partial derivatives of f (at the DFE Q_0) are given by:

$$\frac{\partial^2 f_{k+1}}{\partial x_1\partial x_5} = \frac{\beta_F}{K_F}p_k, \frac{\partial^2 f_{k+1}}{\partial x_1\partial x_7} = \frac{\beta_E}{K_E}p_k, \frac{\partial^2 f_{k+1}}{\partial^2 x_2} = \frac{-2\beta^*{}_I p k}{S_0},$$
$$\frac{\partial^2 f_{k+1}}{\partial x_2\partial x_3} = \frac{-2\beta^*{}_I p_k}{S_0}, \frac{\partial^2 f_{k+1}}{\partial x_2\partial x_4} = \frac{-\beta^*{}_I p_k}{S_0}$$
$$\frac{\partial^2 f_{k+1}}{\partial^2 x_3} = \frac{-2\beta^*{}_I p_k}{S_0} \qquad \text{and} \qquad \frac{\partial^2 f_{k+1}}{\partial x_3\partial x_4} = \frac{-\beta^*{}_I p_k}{S_0} \text{ for } k \in \{1, 2\}.$$

It then follows that

$$\begin{aligned} a &= v_2\sum_{j,i=1}^{8} u_i u_j\frac{\partial^2 f_2}{\partial x_i\partial x_j} + v_3\sum_{j,i=1}^{8} u_i u_j\frac{\partial^2 f_3}{\partial x_i\partial x_j} \\ &= -v_2 u_2^2\left[\frac{\zeta_1\zeta_5\beta_F}{K_F} + \frac{\zeta_1\zeta_7\beta_E}{K_E} + \frac{2\beta_I^*}{S_0} + \frac{2\zeta_3\beta_I^*}{S_0} + \frac{\zeta_2\beta_I^*}{S_0}\right](p_1 + p_2\Gamma_3) < 0. \end{aligned}$$

Thus, $a < 0$ and $b > 0$. So (by Theorem 4, Item(4)) we have established the result about the local stability of the endemic equilibrium of model system (7). We point out that this result holds for $\mathcal{R}_0 > 1$ but close to 1. This achieves the proof.

References

[1] WHO. Choléra. 2014. http://www.who.int/mediacentre/factsheets/fs107/fr/.
[2] JANNY T. Cholera epidemic in africa: analysis of a multifactorial etiology. National School of Public Health; 2014. Master Thesis.
[3] Reidl J, Klose KE. Vibirio cholerae and cholera : out of the water and into the host. FEMS Microbiol Rev 2002;26:125–39.
[4] Libonati JP, Snyder MJ, Wenzel RP, Cash RA, Music SI, Hornick RB. Response of man to infection with vibrio cholerae: clinical, serologic, and bacteriologic responses to a known inoculum. J Infect Dis 1974;129:45–52.
[5] Grimes DJ, Roszak DR, Huq A, Colwell RR, Brayton PR, Palmer LM. Viable, but non-culturable vibrio cholerae and related pathogens in the environment: implication forrelease of genetically engineered microorganisms. Biotechnology 1985;3:817–20.
[6] Xu HS. Survival and viability of non-culturable escherichia coli and vibrio cholerae in the estuarine and marine environment. Microb Ecol 1982;8:313–23.
[7] Roszak DB, Colwell RR. Survival strategies of bacteria in the natural environment. Microb Ecol 1987;51:365–79.
[8] Chava K, Colwell RR, Carroll JW, Mateescu MC, Bej AK. Response and tolerance of toxigenic vibro cholerae o1 to cold temperatures. Int J General Mol Microbiol 2011;79:377–84.
[9] Rahman R, Ali A, Chowdhury MA, Parveen S, Sack DA, Huq A, Colwell RR, Russek-Cohen E. Detection of vibrio cholerae o1 in the aquatic environment by fluorescent-monoclonal antibody and culture methods. Appl Environ Microbiol 1990;56:2370–3.
[10] Mukundan U, Jesudason MV, Balaji V, Thomson CJ. Ecological study of vibrio cholerae in vellore. Epidemiol Infect 2000;124:201–6.
[11] Small EB, Huq MI, Huq A, West PA, Colwell RR. Influence of water temperature, salinity, and ph on survival and growth of toxigenic vibrio cholerae serovar o1 associated with live copepods in a laboratory microcosms. Appl Environ Microbiol 1984;48:420–4.
[12] Morris JG, Calderwood SB, Camilli A, Nelson EJ, Harris JB. Cholera transmission : the 443 host, pathogen and bacteriophage dynamics. Nat Rev Microbiol 2009;7:693–702.
[13] de Magny GC, Mozumder P, Grim CJ, Hasan NA, Naser MM, Alam M, Sack RB, Huq A, Colwell RR. Role of zooplankton diversity in vibrio cholerae population dynamics and in the incidence of cholera in the bangladesh sundarbans. Appl Environ Microbiol 2016;77(17):125–6132. doi:10.1128/AEM.01472-10.
[14] Kirschner AK, et al. Rapid growth of planktonic vibrio cholerae non-o1/non-o139 strains in a large alkaline lake in austria: dependence on temperature and dissolved organic carbon quality. Appl Environ Microbiol 2008;74:2004–15.
[15] Huq A, et al. Ecological relationships between vibrio cholerae and planktonic crustacean copepods. Appl Environ Microbiol 1983;45:275–83.
[16] Chowdhury MA, Huq A, Xu B, Madeira FJ, Colwell RR. Effect of alum on free-living and copepod-associated vibrio cholerae o1 and o139. Appl Environ Microbiol 1997;63:3323–6.
[17] Hunt DE, Gevers D, Vahora NM, Polz MF. Conservation of the chitin utilization pathway in the vibrionaceae. Appl Environ Microbiol 2008;74:44–51.
[18] Dobson AP, Pascual M, Bouma MJ. Cholera and climate : revisiting the quantitative evidence. Microbes Infection 2002;4:237–45.
[19] David J, Smith L, Hartley DM, Morris JG. Hyperinfectivity: a critical element in the ability of v. cholerae to cause epidemics? PLoS Med 2006;3. doi:10.1371/journal.pmed.0030007. E7
[20] Wang J, Gaff H, Smith DL, Morris JG, Mukandavire Z, Liao S. Estimating the basic reproduction number for the 2008–2009 cholera outbreaks in zimbabwe. PNAS 2011;108:8767–72.
[21] Zhou X, Cui J, Wu Z. Mathematical analysis of a cholera model with vaccination. Math Method Appl Sci 2011;34:1711–24.
[22] Cazelle B, DeLara M, Delmas JF, Guegan JF, de Magny GC, Paroissin C. Modeling environmental impacts of plankton reservoirs on cholera population dynamics. ESAIM 2005;14:156–73. doi:10.1051/proc:200501.
[23] Paveri-Fontana SL, Copasso V. A model for the 1973 cholera epidemic in the european mediterranean region. Rev Epidem et Santé Publ 1979;27:121–32.
[24] Codeço CT. Endemic and epidemic dynamics of cholera : the role of the aquatic reservoir. BMC Infect Dis 2001;1:1.
[25] Bayleyegn Y.N.. A mathematical analysis of a model of cholera transmission dynamics. 2009. Master's thesis
[26] Bhunu CP, Mushayabasa S. Is hiv infection associated with an increased risk for cholera? insights from a mathematical model. BioSystems 2012;109:203–13. doi:10.1016/j.biosystems.2012.05.002.
[27] Tchuenche JM, Mwasa A. Mathematical analysis of a cholera model with public health interventions. BioSystems 2011;105:190–200.
[28] Musekwa DH, Nyabadza F, Chiyaka C, Das P, Tripathif A, Mukandavire Z. Modelling and analysis of the effects of malnutrition in the spread of cholera. Math Comput Modell 2011;53:1583–95.
[29] Nyabadza F, Njagarah JBH. A metapopulation model for cholera transmission dynamics between communities linked by migration. Appl Math Comput 2014;241:317–31.
[30] Campus de microbiologie medicale. vibrio. 2015. http://www.microbes-edu.org/etudiant/vibrio.html.
[31] Garnotel E, Morillon M. Cholera. EMC- Maladies Infectieuses 2004;1:67–80.
[32] Thieme H. Convergence results and a poincaré bendixson trichotomy for asymptotically autonomous differential equations. J Math Biol 1992;7:755–67.
[33] World statistics. cameroon. http://www.statistiques-mondiales.com/cameroun.htm.
[34] Ministère de la santé du cameroun, données choléra 1994–2013. 2014.
[35] Pascual M, Bouma M, King A, Ionides EL. In apparent infections and cholera dynamics. Nature 2008;454:877–80.
[36] Rota GC, Birkhoff G. Ordinary differential equations. Ginn: Need ham Heights; 1982.
[37] Schmitt K, Hutson V. Permanence and the dynamics of biological systems. Math Biosci 1982;111:1–71.
[38] Simon CP, Jacquez JA. Qualitative theory of compartmental systems. SIAM 1993;35:43–79.
[39] Watmough J, van den Driessche P. Reproduction numbers and sub-threshold endemic equilibria for compartmental models of disease transmission. Math Bios 2002;180. 29–28
[40] Plemmons R.J., Berman A. Nonnegative matrices in the mathematical sciences. SIAM 1994.
[41] Kamgang JC. Contribution à la stabilité des systèmes mécaniques, contribution à l'étude de la stabilité des modèles épidémiologiques. University of Metz; 2003. Phd thesis.
[42] Song B, Castillo-Chavez C. Dynamical models of tuberculosis and their applications. Math Bio Sci Eng 2004;1:361–404.
[43] Carr J. Applications centre manifold theory. Springer-Verlag; 1981.
[44] Ray CJ, Marino S, Hogue IB, Kirschner DE. A methodology for performing global uncertainty and sensitivity analysis in systems biology. J Theor Biol 2008;254:178–96.
[45] Bouma MJ, Pascual M. Seasonal and interannual cycles of endemic cholera in bengal 1891–1940 in relation to climate and geography. Hydrobiologia 2001;460:147–56.
[46] Colwell RR. Global climate and infectious disease : the cholera paradigm. Science 1996;274:2025–31.
[47] Huq A, Lipp EK, Colwell RR. Effects of global climate on infectious disease: the cholera model. Clin microbiol Rev Sci 2002;15:757–70.
[48] Bouma MJ, Pascual M, Dobson AP. Cholera and climate: revisiting the quantitative evidence. Microbes Infect 2002;4:237–45.
[49] Colwell RR, Huq A. Environmental reservoir of vibrio cholerae the causative agent of cholera. Ann NY Acad Sci 1994;740:44–54.
[50] Sallet G, Kamgang JC. Computation of threshold conditions for epidemiological models and global stability of the disease-free equilibrium (DFE). Math Biosci 2008;213:1–12.